

Saturated Linkers in Two-Dimensional Covalent Organic Frameworks Boost their Luminescence

Meijia Yang, Hiroki Hanayama, Long Fang, Matthew A. Addicoat, Yunyu Guo, Robert Graf, Koji Harano, Jun Kikkawa, Enquan Jin*, Akimitsu Narita* and Klaus Müllen*

Dr. M. Yang, Dr. R. Graf, Prof. Dr. E. Jin, Prof. Dr. A. Narita and Prof. Dr. K. Müllen
Max Planck Institute for Polymer Research
Ackermannweg 10, 55128, Mainz, Germany.
E-mail: muellen@mpip-mainz.mpg.de

Y. Guo and Prof. Dr. E. Jin
State Key Laboratory of Inorganic Synthesis and Preparative Chemistry,
College of Chemistry and International Center of Future Science, Jilin University
Changchun 130012, P.R. China.
E-mail: enquanjin@jlu.edu.cn;

Dr. H. Hanayama and Prof. Dr. A. Narita
Organic and Carbon Nanomaterials Unit, Okinawa Institute of Science and
Technology Graduate University
Kunigami-gun, Okinawa 904-0495, Japan.
E-mail: akimitsu.narita@oist.jp

L. Fang
Key Laboratory for Polymeric Composite and Functional Materials of Ministry of
Education, School of Chemistry, Sun Yat-sen University
Guangzhou 510275, Guangdong Province, China.

Prof. Dr. M. A. Addicoat
School of Science and Technology, Nottingham Trent University
Clifton Lane, Nottingham NG11 8NS, UK.

Dr. K. Harano and Dr. J. Kikkawa
Center for Basic Research on Materials, National Institute for Materials Science
1-1 Namiki, Tsukuba, Ibaraki 305-0044, Japan.

Table of Contents

Section A: General Materials and Methods

Section B: Synthetic Details

Section C: Characteristics

Section D: Fluorescence Sensor Experiments

Section E: References

Section A: General Materials

N,N-dimethylacetamide (DMAc), 1,4-dioxane, acetic acid (HAc), *n*-butanol (*n*-BuOH), 1,2-dichlorobenzene (*o*-DCB), *N,N*-dimethylformamide (DMF), dichloromethane (DCM) tetrahydrofuran (THF), triethylamine (TEA), meistylene, acetone and methanol were purchased from Sigma - Aldrich company. 1,3,5-triformylbenzene (TFB), *p*-phenylenediamine (PDA), tetrakis(triphenylphosphine)palladium (Pd(PPh₃)₄), 4-bromobenzaldehyde, potassium carbonate (K₂CO₃), picric acid (PA) and phenylglyoxylic acid (PGA) were purchased from Tokyo chemical industry Co., Ltd. (TCI). NaClO₄, Mg(ClO₄)₂, Cu(ClO₄)₂, Zn(ClO₄)₂, Ni(ClO₄)₂, Co(ClO₄)₂, Fe(ClO₄)₂ and Fe(ClO₄)₃ were used for the detection of diverse metal ions. The 1,3,5-Tris(4-formylphenyl)benzene (TFPB),¹ 1,3,6,8-tetrakis(4-formylphenyl)pyrene (TFPPy),²⁻⁷ 2,5,8,11-tetrakis(4,4,5,5-tetramethyl-1,3,2-dioxaborolan-2-yl)perylene⁸, 2,5,8,11-tetrakis(4-formylphenyl)perylene (TFPPery),⁹ and TFPPy-PDA COF¹⁰ were synthesized according to reported methods. The 4,4',4'',4'''-(ethene-1,1,2,2-tetrayl)tetrabenzaldehyde (ETTA) was purchased from AbaChemScene company. Unless otherwise noted, all reagents were used without further purification. *Trans*-1,4-diaminocyclohexane (CHDA) was obtained from Tokyo chemical industry Co., Ltd. (TCI) and recrystallized by DCM and methanol for several times before it is applied.

Characterization Methods

All reactions were performed under Ar atmosphere or with Schlenk line techniques. Thin layer chromatography (TLC) was carried out on silica gel-coated aluminum sheets with an F254 indicator, and column chromatography separation was conducted with silica gel (particle size of 0.063–0.200 mm). High-resolution mass spectra (HR-MS) were recorded on a Bruker Reflex II-TOF spectrometer by matrix-assisted laser decomposition/ionization (MALDI) using 7,7,8,8-tetracyanoquinodimethane (TCNQ) as matrix calibrated against poly(ethylene glycol). Nuclear magnetic resonance (NMR) spectra were recorded using Bruker DPX 300 MHz NMR spectrometers, and chemical shifts (δ) were expressed in ppm relative to the residual of solvents (C₂D₂Cl₄, 1H: 6.00

ppm). Coupling constants (J) were expressed in Hertz. Fourier transform infrared (FT-IR) spectroscopy was detected on a Bruker TENSOR II FTIR spectrometer with a scan number of 64, and the background was subtracted. Each elemental analysis (EA) was obtained on Elementar Vario EL elemental analyzer. Powder X-ray diffraction (PXRD) measurements were performed on a Rigaku Smart Lab X-ray diffractometer by putting powder on the glass substrate, from $2\theta = 1.5^\circ$ up to 30° with 0.02° increment. Nitrogen sorption isotherms were recorded on a Micrometrics TriStar II Plus gas sorption instrument. Before measurement, powder samples were degassed in a vacuum at 120°C over 6 h. The Pore volume was calculated using the cylindrical quench solid density functional theory (QSDFT) model from the nitrogen gas sorption curve. Field emission scanning electron microscopy (FE SEM) was measured on the scanning electron microscopy (Hitachi S-4800, Japan) with a cold field emission gun working at 10.0 kV acceleration voltage. Thermogravimetric analysis (TGA) measurement was performed under nitrogen (50 mL/min) with a temperature increase from 50°C to 800°C at a rate of $10^\circ\text{C}/\text{min}$. High-resolution transmission electron microscope (HR-TEM) analysis was recorded on ThermoFisher Titan G2 electron microscope, operated at 200 kV. A Fischione 2020 single tilt tomography holder was used for this work. ^{13}C cross-polarization magic-angle spinning nuclear magnetic resonance (CP-MAS-NMR) spectra were characterized with a Bruker Avance III console operating at 700.25 MHz ^1H Larmor frequency, using a double-resonance MAS probe supporting zirconia MAS rotors with 2.5 mm outer diameter spinning at 25 kHz MAS frequency. UV-vis absorption spectra were performed on a Perkin-Elmer Lambda 900 spectrometer. The Ocean optics spectrograph (CDS-600, Labsphere, America) was employed to detect the luminescent spectra under different stimuli. The fluorescence intensity vs. time curve was carried out on a FLS920-Combined Time Resolved & Steady State Fluorescence Spectrometer (Edinburgh Instruments) employing the Xe lamp (Xe 900) as the excitation source and RP928 photomultiplier tube as the detector at room temperature. The time-dependent photoluminescence (PL) decay dynamics of samples were stimulated by picosecond diode laser pulses (EPL-405). The pulse width, wavelength, and repetition rate were 58.8 ps, 405 nm, and 40.0 kHz, respectively.

Sensor experiments were carried out by gradually adding THF solutions of metal ions, PA and PGA (1.5×10^{-2} M for metal ions, 6×10^{-4} M for PA, and 1×10^{-3} M for PGA) into ETTA-CHDA-COF suspensions in THF ($50 \mu\text{g mL}^{-1}$, 3.0 mL) at intervals of 5 mins. Finally, fluorescence spectra with different intensity were recorded at room temperature excited by the same wavelength of 360 nm. Besides, a certain amount of extra THF solvent was added to the quartz cell to make the total solution volume constant (3 mL) so that the concentration of COF stays the same in different measurements. All the changes of luminescence spectra in the detection of Fe^{3+} , PA and PGA occurred immediately after the addition of each analyte. Each fluorescence spectra of different detection limit was measured at least for three times to get the reliable value.

Photoluminescence Quantum Yield (PLQY) Measurement

PLQY was recorded with a HORIBA Jobin-Yvon Fluorolog 3-22 Tau-3 with an intergrating sphere (F-3810 from Horiba Jobin Yvon) in the air atmosphere using the method described in the literature.¹¹ Notably, one sample's spectra were recorded with the same excitation and emission monochromator bandpass (slits opening). Besides, most of the excitation profiles were recorded through a neutral gauze density (ND) filter(s) to avoid exceeding the intensity of the excitation profiles, and the ND value of the filter used was then taken into account in the calculation of the absorbed value, giving this last equation: The PLQY is defined as

$$\Phi_{\text{pL}} = \frac{\text{emittted photons}}{\text{absorbed photons}} \text{ ND}_{\text{selected}}$$

Computational Details

Molecular modeling and Pawley refinement were carried out using Reflex, a software package for crystal determination from XRD pattern as implemented in Materials Studio (MS) modeling version 4.4 (Accelrys Inc.).¹²⁻¹³ Pawley refinement was utilized to optimize the lattice parameters iteratively until the R_{P} and R_{WP} values converge. Geometries of a monolayer, AA and AB stacking for TFB-CHDA COF,

TFPB-CHDA COF, TFPPy-CHDA COF, TFPPery-CHDA COF, TFPPery-PDA COF, and ETTA-CHDA COF were calculated using density functional tight binding (DFTB) implemented in DFTB⁺ version 20.1.¹⁴ All-atom pairs were calculated via standard parameters from the mio-0-1 parameter set.¹⁵

High-Resolution Transmission Electron Microscopy (HR-TEM)

For the sample preparation, ETTA-CHDA COF, TFPPery-CHDA COF, and TFB-CHDA COF was bath-sonicated in dichloromethane or THF (0.01 mg/mL), respectively, for 5 min. Then, 10 µL of the suspension was placed onto a microgrids and the excessive amount of solvent was blotted by a filter paper. This procedure was repeated for 3 times. The microgrid was dried under reduced pressure for 3 hours before observation by the electron microscopy. TEM samples were prepared by using a TEM grid precoated with a lacy microgrid (NS-C15, pore size 1.5–8 µm) was purchased from Okenshoji Co., Ltd. For low electron dose imaging, we used a CVD-grown monolayer graphene-coated quantifoil gold grids, with a hole size of 2 µm and space between the hole of 4 µm, were purchased from Graphenea.

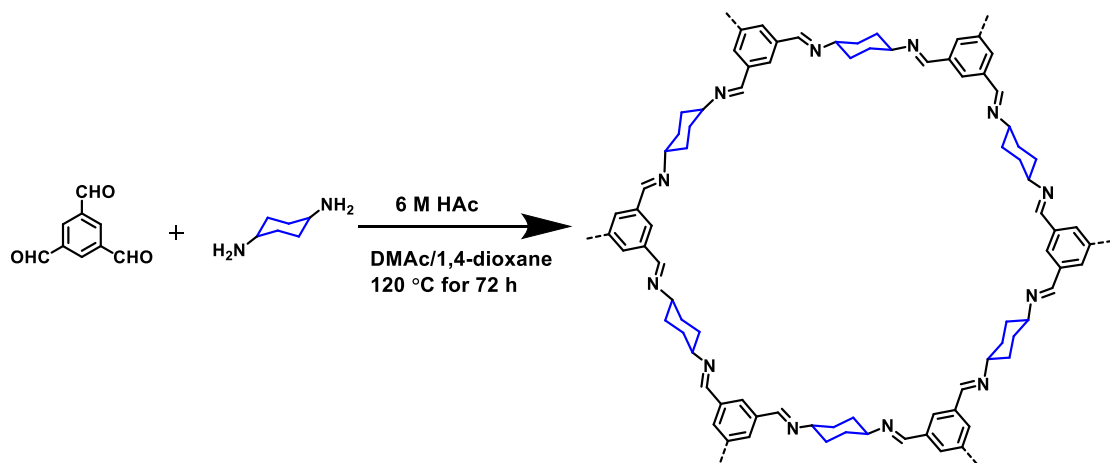
HR-TEM imaging of ETTA-CHDA COF, TFPPery-CHDA COF, and TFB-CHDA COF was carried out on Titan G2 electron microscope (Thermo Fischer Scientific, Inc., operated at 200 kV) equipped with a Schottky XFEG electron source, S-TWIN objective lens, image Cs-corrector (CEOS GmbH), with Gatan 2k×2k UltrascanXP1000 camera (Gatan, Inc.). A Fischione 2020 single tilt tomography holder was used for this work. The raw TEM images were collected as a .dm4 format file on DigitalMicrograph software (Gatan, Inc.) and further processed using ImageJ 1.53c software. The HR-TEM images were filtered using a bandpass filter (filtering structures smaller than 3 pixels and larger than 40 pixels, tolerance of direction: 5%). TEM simulation images were generated by using a multi-slice procedure implemented in the ELBis software.¹⁶

Low electron dose imaging of ETTA-CHDA COF was carried out on Themis Z

(Thermo Fischer Scientific Inc., operated at 300 kV) equipped with Gatan 4k×4k K2 direct electron detection camera (Gatan, Inc.) operated at a counting mode. A FEI double tilt holder was used for this work. Image collection was conducted with an electron dose rate of $2 \text{ e}^- \text{ \AA}^{-2} \text{ s}^{-1}$ to suppress beam-induced deformation of the crystalline samples. Fifty successive images collected at an exposure time of 0.5 s were aligned and superimposed by using a drift correction function implemented in the DigitalMicrograph software. To extract a periodic feature of the crystals, the images were processed by the Local 2D Wiener filter of HREM Filters Pro (HREM Research Inc.) implemented as DigitalMicrograph plugin.

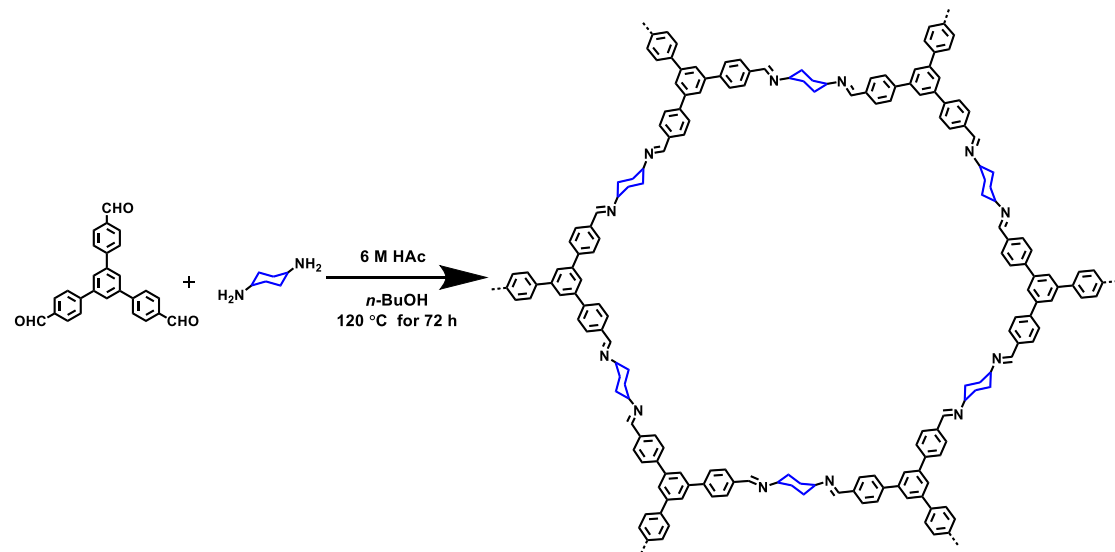
Section B: Synthetic Details

Scheme S1. Synthetic route towards TFB-CHDA COF.



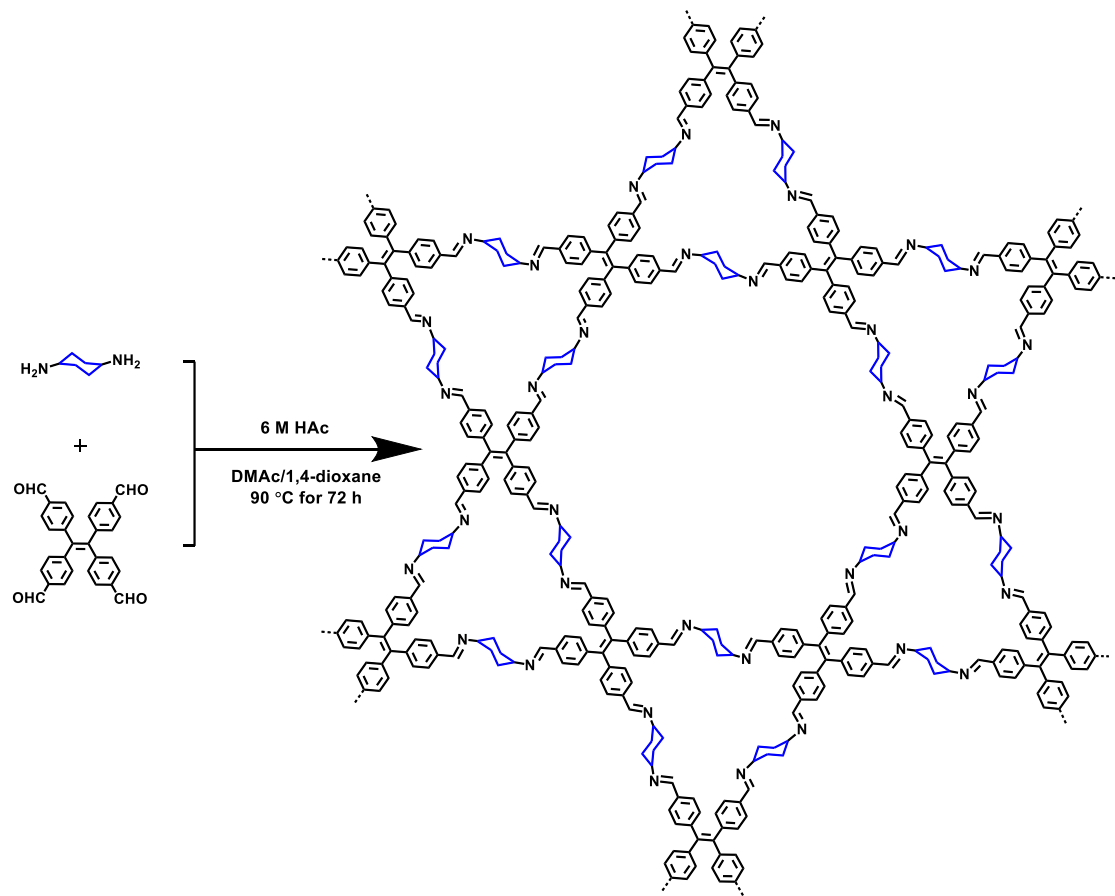
A microwave tube (15 mL) placed with TFB (19.0 mg, 0.117 mmol), CHDA (20.0 mg, 0.175 mmol), DMAc (2.4 mL), 1,4-dioxane (0.6 ml), and 6 M HAc (50 μL) was sonicated for 30 s and degassed through three freeze-pump-thaw cycles before sealing under vacuum. The tube was then sealed at 120°C for 3 days. After cooling to room temperature, the white-colored precipitate was filtered and washed with degassed THF and acetone several times. The powder was dried under vacuum at 60°C for 12 h to produce TFB-CHDA COF in 87% yield. Elemental analysis: calculated C (79.61%), H (8.02%), N (12.38%) and observed C (71.74%), H (7.29%), N (13.06%).

Scheme S2. Synthetic route towards TFPB-CHDA COF.



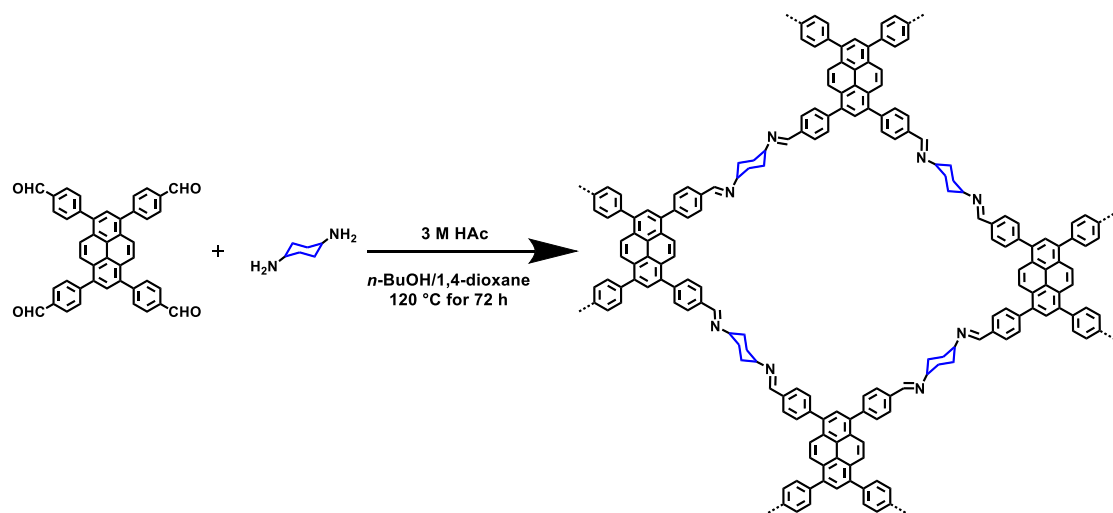
A microwave tube (15 mL) placed with TFPB (20.0 mg, 0.051 mmol), CHDA (17.5mg, 0.0765 mmol), *n*-BuOH (3 mL), and 6 M HAc (50 μ L) was sonicated for 30 s and degassed through three freeze-pump-thaw cycles before sealing under vacuum. The tube was then sealed at 120 °C for 3 days. After cooling to room temperature, the white-colored precipitate was filtered and washed with degassed THF and acetone several times. The powder was dried under vacuum at 60 °C for 12 h to produce TFPB-CHDA COF in 91% yield. Elemental analysis: calculated C (87.19%), H (6.65%), N (6.16%) and observed C (84.17%), H (2.79%), N (7.09%).

Scheme S3. Synthetic route towards ETTA-CHDA COF.



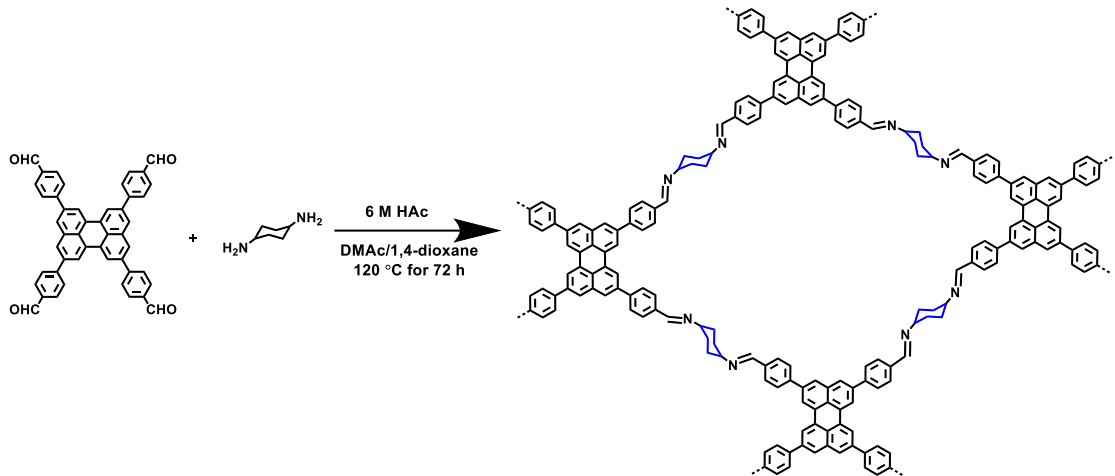
A microwave tube (15 mL) placed with ETTA (19.0 mg, 0.043 mmol), CHDA (10.0 mg, 0.086 mmol), DMAc (0.8 mL), and 1,4-dioxane (0.2 mL) was sonicated for 30 s and degassed through three freeze-pump-thaw cycles before sealing under vacuum. Afterward, 6 M HAc (20 μL) was added to the tube and then sealed at 90°C for over 3 days. After cooling to room temperature, the light yellow-colored precipitate was filtered and washed with degassed THF and acetone several times. The powder was dried with nitrogen gas flow to produce ETTA-CHDA COF in 82% yield. Elemental analysis: calculated C (84.53%), H (6.08%), N (9.39%) and observed C (79.52%), H (6.66%), N (8.52%).

Scheme S4. Synthetic route towards TFPPy-CHDA COF.



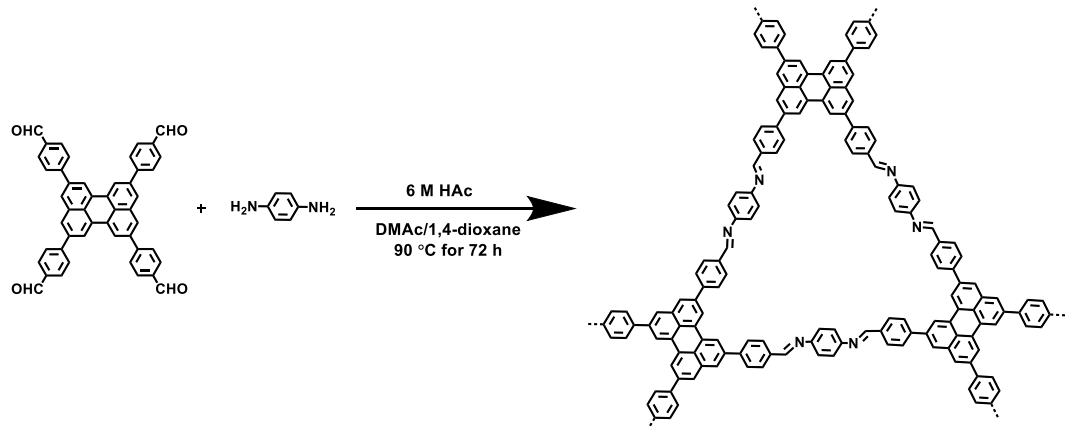
A microwave tube (15 mL) placed with TFPPy (27.1 mg, 0.043 mmol), CHDA (10.0 mg, 0.086 mmol), *n*-BuOH (1.2 mL), and 1,4-dioxane (0.3 mL) was sonicated for 30 s and degassed through three freeze-pump-thaw cycles before sealing under vacuum. Afterward, 3 M HAc (50 μ L) was added to the tube and then sealed at 120 °C for over 3 days. After cooling to room temperature, the yellow-colored precipitate was filtered and washed with degassed THF and acetone several times. The powder was dried under vacuum at 60 °C for 12 h to produce TFPPy-CHDA COF in 93% yield. Elemental analysis: calculated C (87.23%), H (5.49%), N (7.23%) and observed C (82.87%), H (6.23%), N (10.81%).

Scheme S5. Synthetic route towards TFPPery-CHDA COF.



A microwave tube (15 mL) placed with TFPPery (29.3 mg, 0.043 mmol), CHDA (9.4 mg, 0.086 mmol), DMAc (1.2 mL), 1,4-dioxane (0.3 mL), and 6 M HAc (100 μ L) was sonicated for 30 s and degassed through three freeze-pump-thaw cycles before sealing under vacuum. Afterward, the tube and the solution were sealed at 120 °C for over 3 days. After cooling to room temperature, the orange-colored precipitate was filtered and washed with degassed THF and acetone several times. The powder was dried under vacuum at 60 °C for 12 h to produce TFPPery-CHDA COF in 91% yield. Elemental analysis: calculated C (87.77%), H (5.40%), N (6.82%) and observed C (82.11%), H (5.92%), N (5.08%).

Scheme S6. Synthetic route towards TFPPery-PDA COF.



A microwave tube (15 mL) placed with TFPPery (29.3 mg, 0.043 mmol), PDA (10.0 mg, 0.086 mmol), DMAc (1.25 mL), 1,4-dioxane (1.25 mL), and 6 M HAc (100 μ L) was sonicated for 30 s and degassed through three freeze-pump-thaw cycles before sealing under vacuum. After that, the solution was then sealed at 90 °C for over 3 days. After cooling to room temperature, the dark red-colored precipitate was filtered and washed with degassed THF and acetone several times. The powder was dried under vacuum at 60 °C for 12 h to produce TFPPy-PDA COF in 93% yield. Elemental analysis: calculated C (88.64%), H (4.46%), N (6.89%) and observed C (82.91%), H (5.22%), N (5.60%).

Section C: Characteristics

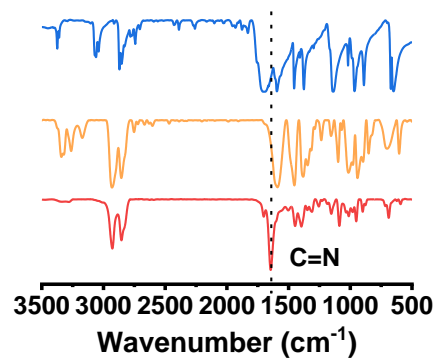


Figure S1. FT-IR spectra of TFB (blue), CHDA (yellow), and TFB-CHDA COF (red), respectively.

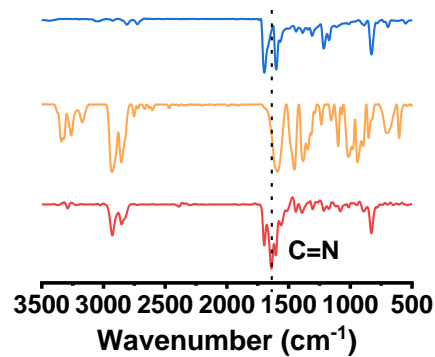


Figure S2. FT-IR spectra of TFPB (blue), CHDA (yellow), and TFPB-CHDA COF (red), respectively.

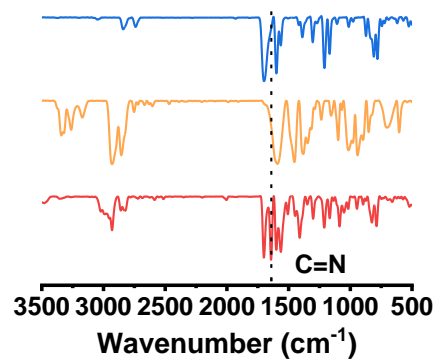


Figure S3. FT-IR spectra of ETTA (blue), CHDA (yellow), and ETTA-CHDA COF (red), respectively.

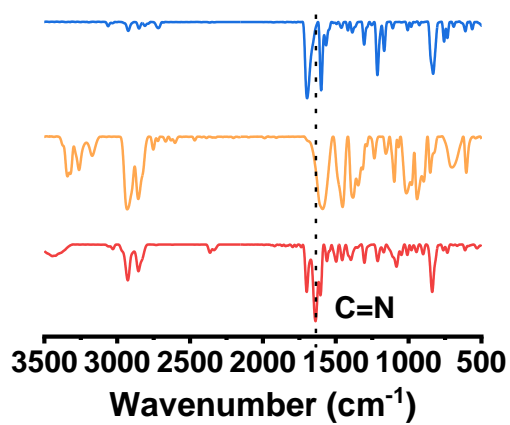


Figure S4. FT-IR spectra of TFPY (blue), CHDA (yellow), and TFPY-CHDA COF (red), respectively.

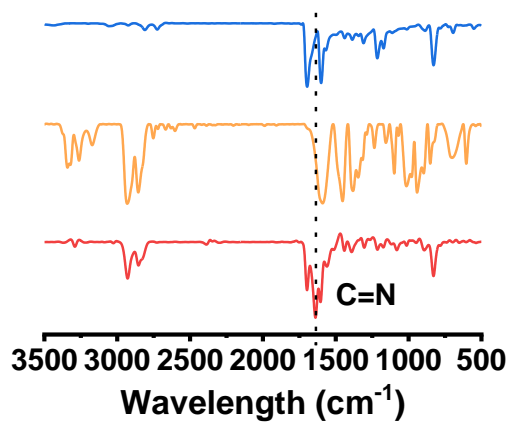


Figure S5. FTIR spectra of TFPY (blue), CHDA (yellow), and TFPY-CHDA COF (red), respectively.

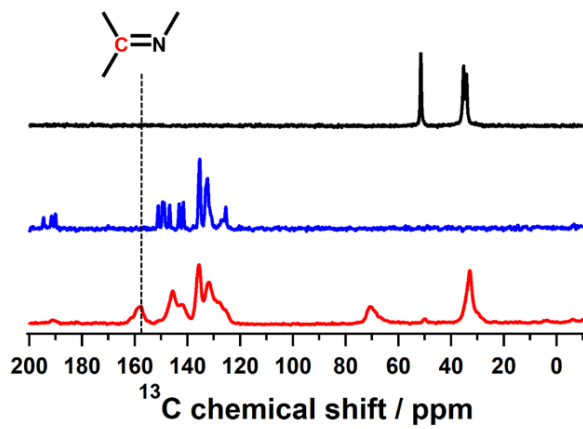


Figure S6. ¹³C CP-MAS-NMR spectra of CHDA (black), ETTA (blue) and ETTA-CHDA COF (red).

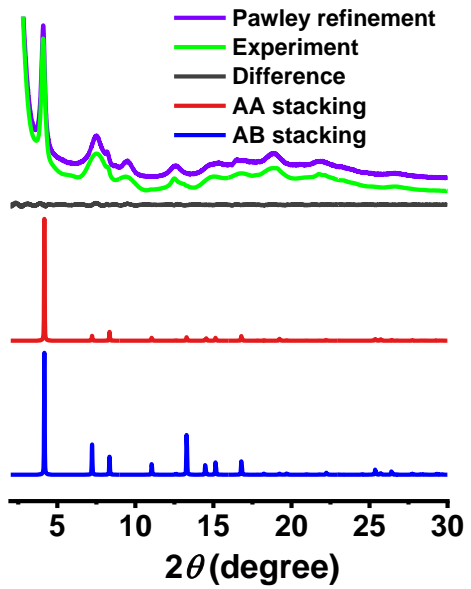


Figure S7. PXRD of TFB-CHDA COF analyzed by different simulated patterns: slipped AA stacking mode (red) and AB eclipsed stacking mode (blue) with the experimental pattern (green) combined Pawley refined pattern (purple) and the difference (gray) between experimental and stimulated patterns.

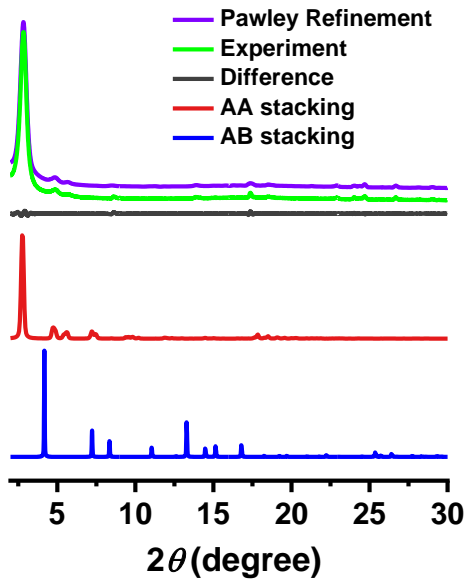


Figure S8. PXRD of TFPB-CHDA COF analyzed by different simulated patterns: slipped AA stacking mode (red) and AB eclipsed stacking mode (blue) with the experimental pattern (green) combined Pawley refined pattern (purple) and the difference (gray) between experimental and stimulated patterns.

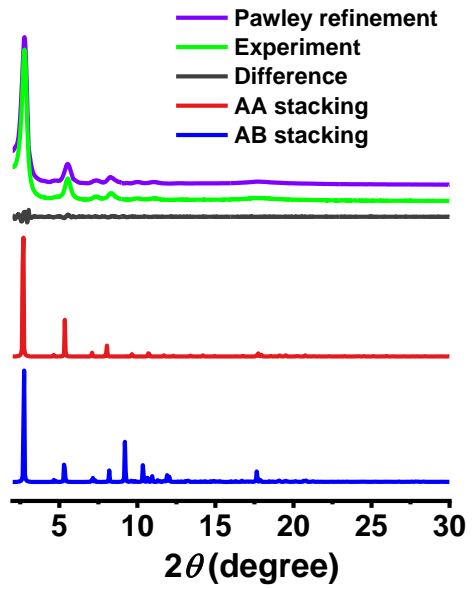


Figure S9. PXRD of ETTA-CHDA COF analyzed by different simulated patterns: slipped AA stacking mode (red) and AB eclipsed stacking mode (blue) with the experimental pattern (green) combined Pawley refined pattern (purple) and the difference (gray) between experimental and stimulated patterns.

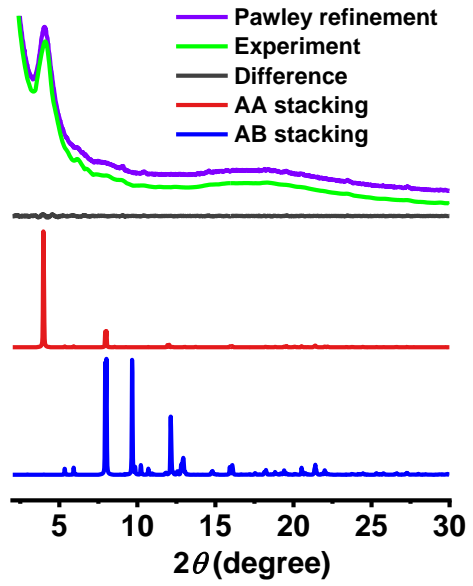


Figure S10. PXRD of TFPPy-CHDA COF analyzed by different simulated patterns: slipped AA stacking mode (red) and AB eclipsed stacking mode (blue) with the experimental pattern (green) combined Pawley refined pattern (purple) and the difference (gray) between experimental and stimulated patterns.

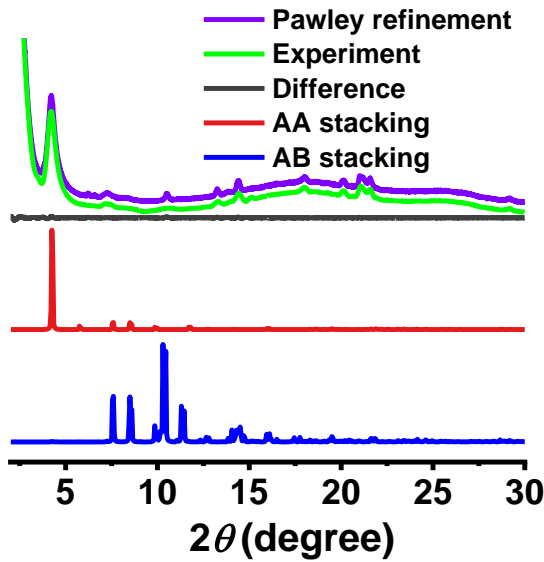


Figure S11. PXRD of TFPPer-CHDA COF analyzed by different simulated patterns: slipped AA stacking mode (red) and AB eclipsed stacking mode (blue) with the experimental pattern (green) combined Pawley refined pattern (purple) and the difference (gray) between experimental and stimulated patterns.

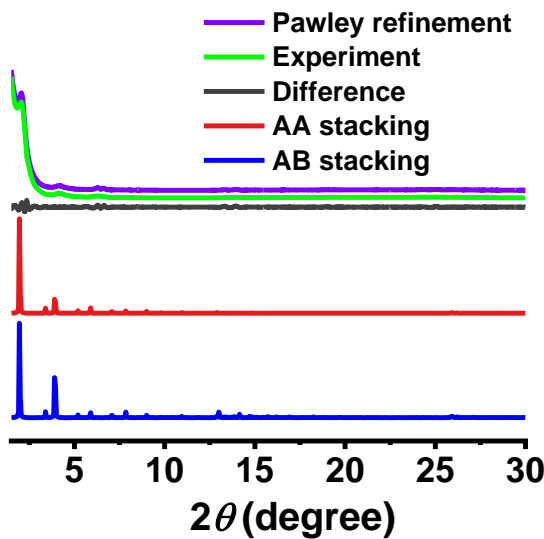


Figure S12. PXRD of TFPPer-PDA COF analyzed by different simulated patterns: slipped AA stacking mode (red) and AB eclipsed stacking mode (blue) with the experimental pattern (green) combined Pawley refined pattern (purple) and the difference (gray) between experimental and stimulated patterns.

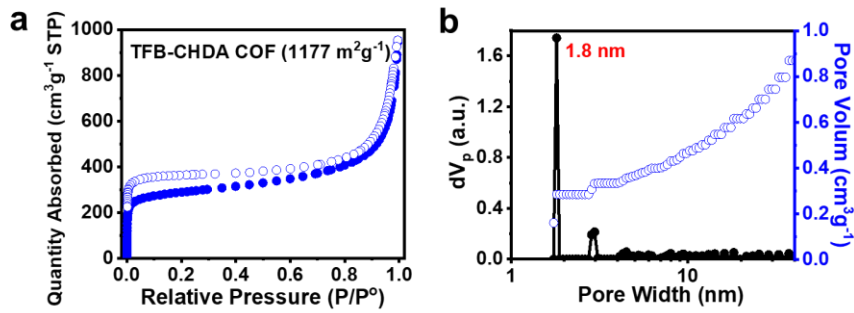


Figure S13. (a) Nitrogen adsorption-desorption isotherms curves of TFB-CHDA COF.
(b) The pore size distribution and corresponding cumulative pore volume were stimulated by fitting the nitrogen adsorption-desorption isotherms curves at 77 K with the QSDFT model.

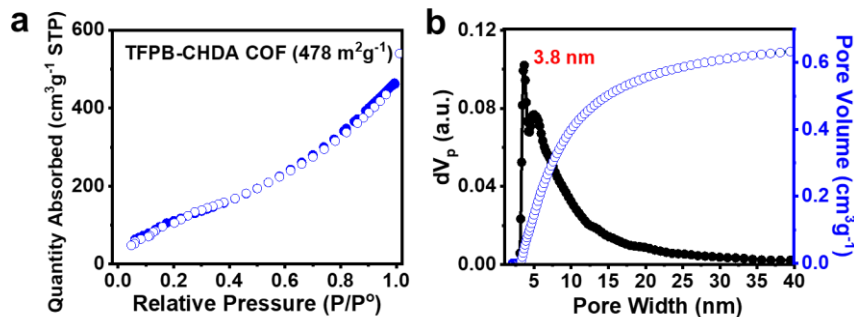


Figure S14. (a) Nitrogen adsorption-desorption isotherms curves of TFPB-CHDA COF.
(b) The pore size distribution and corresponding cumulative pore volume were stimulated by fitting the nitrogen adsorption-desorption isotherms curves at 77 K with the QSDFT model.

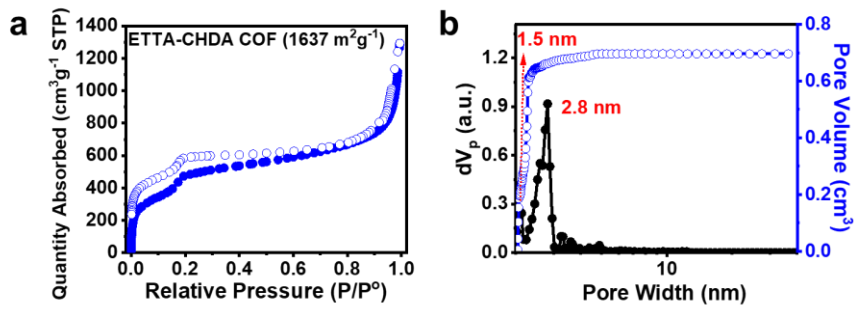


Figure S15. (a) Nitrogen adsorption-desorption isotherms curves of ETTA-CHDA COF.
(b) The pore size distribution and corresponding cumulative pore volume were stimulated by fitting the nitrogen adsorption-desorption isotherms curves at 77 K with the QSDFT model.

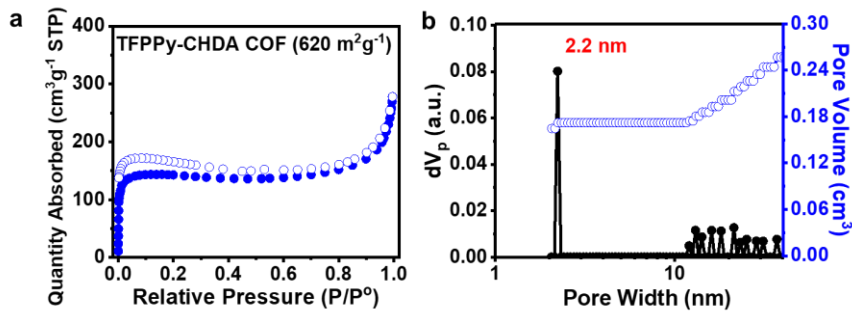


Figure S16. (a) Nitrogen adsorption-desorption isotherms curves of TFPPy-CHDA COF. (b) The pore size distribution and corresponding cumulative pore volume were stimulated by fitting the nitrogen adsorption-desorption isotherms curves at 77 K with the QSDFT model.

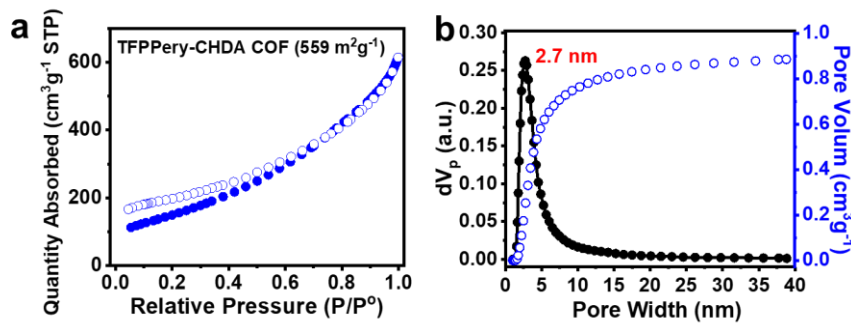


Figure S17. (a) Nitrogen adsorption-desorption isotherms curves of TFPPery-CHDA COF. (b) The pore size distribution and corresponding cumulative pore volume were stimulated by fitting the nitrogen adsorption-desorption isotherms curves at 77 K with the QSDFT model.

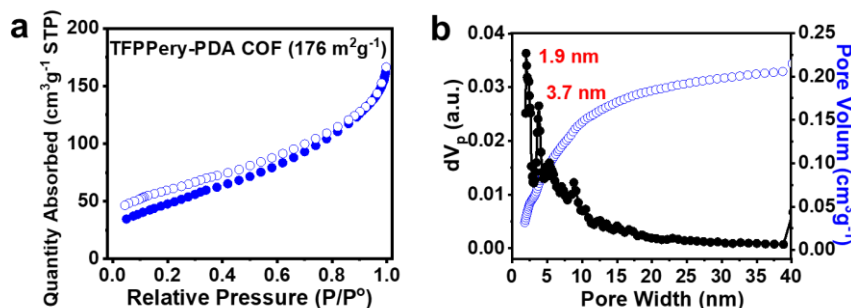


Figure S18. (a) Nitrogen adsorption-desorption isotherms curves of TFPPery-PDA COF. (b) The pore size distribution and corresponding cumulative pore volume were stimulated by fitting the nitrogen adsorption-desorption isotherms curves at 77 K with the QSDFT model.

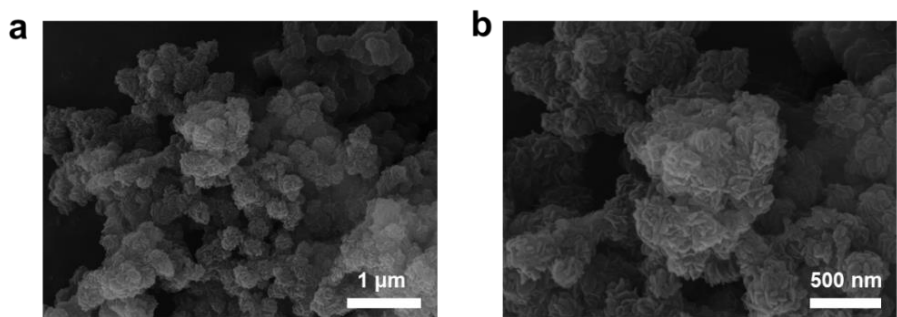


Figure S19. SEM images of TFB-CHDA COF.

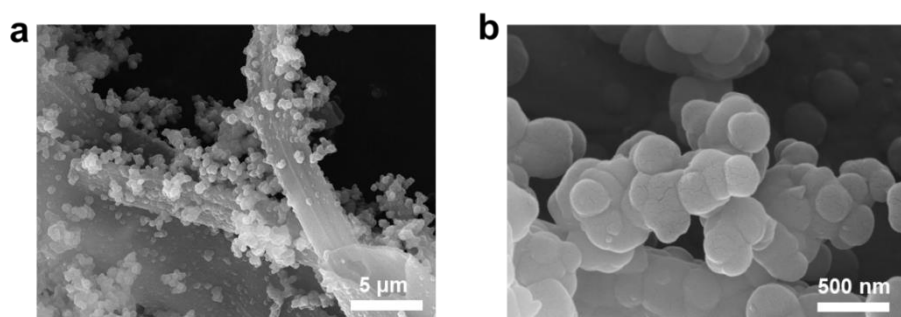


Figure S20. SEM images of TFPB-CHDA COF.

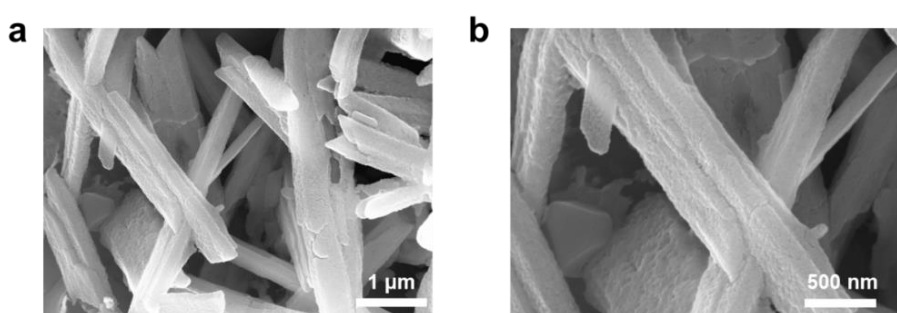


Figure S21. SEM images of ETTA-CHDA COF.

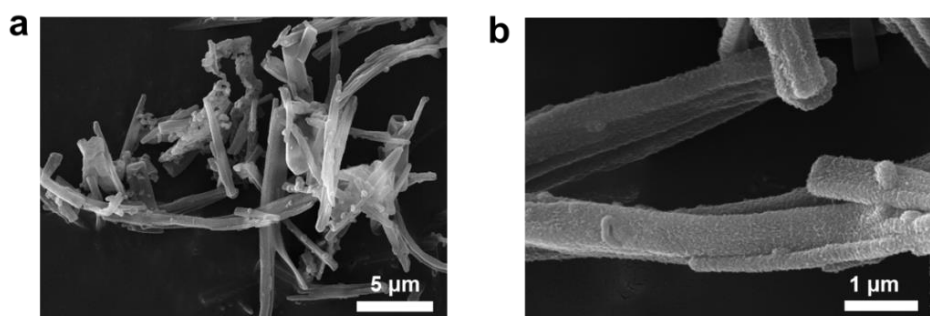


Figure S22. SEM images of TFPPy-CHDA COF.

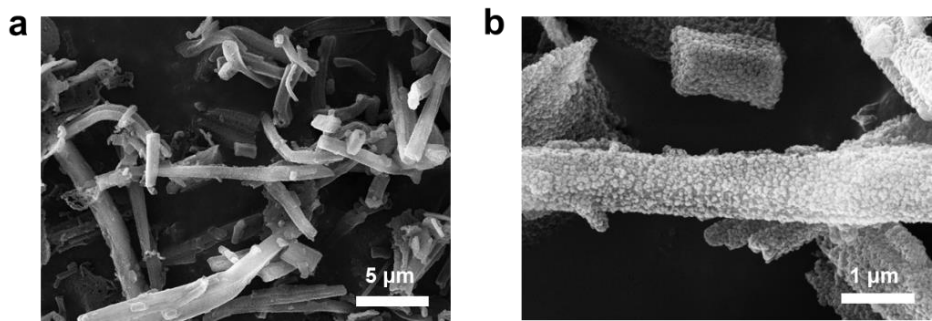


Figure S23. SEM images of TFPPer-CHDA COF.

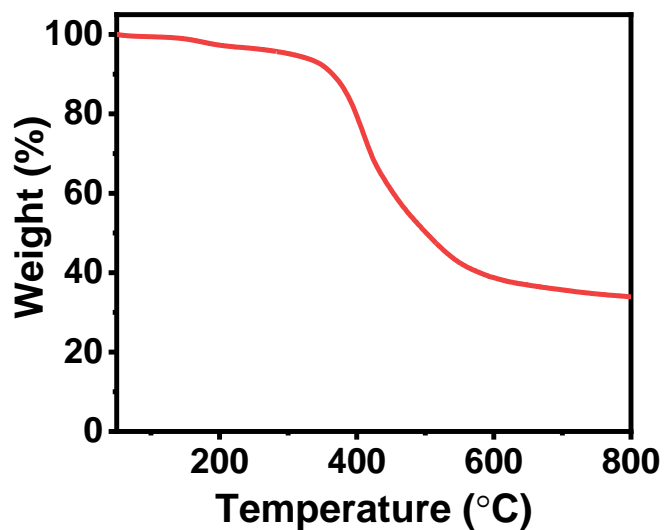


Figure S24. TGA curve of TFB-CHDA COF under nitrogen atmosphere.

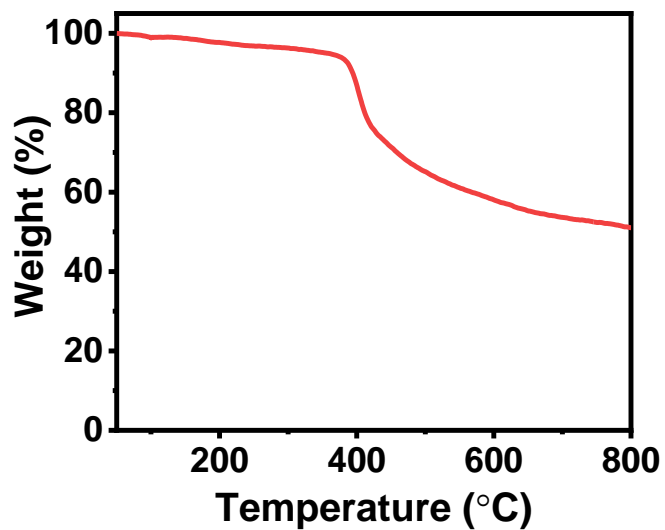


Figure S25. TGA curve of TFPB-CHDA COF under nitrogen atmosphere.

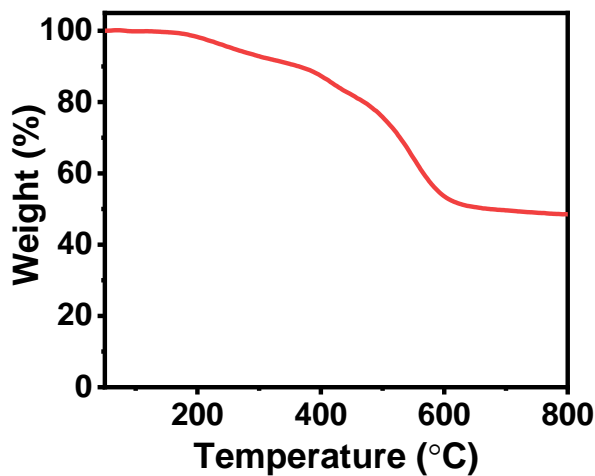


Figure S26. TGA curve of ETTA-CHDA COF under nitrogen atmosphere.

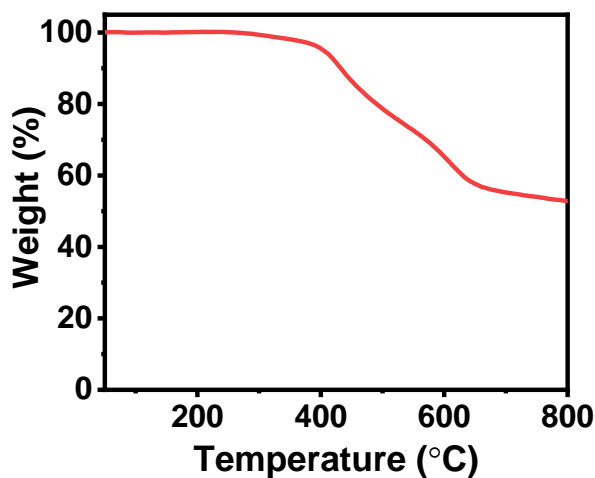


Figure S27. TGA curve of TFPPy-CHDA COF under nitrogen atmosphere.

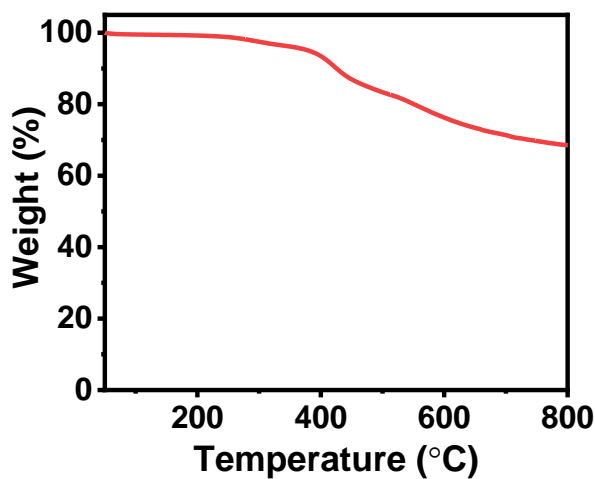


Figure S28. TGA curve of TFPPery-CHDA COF under nitrogen atmosphere.

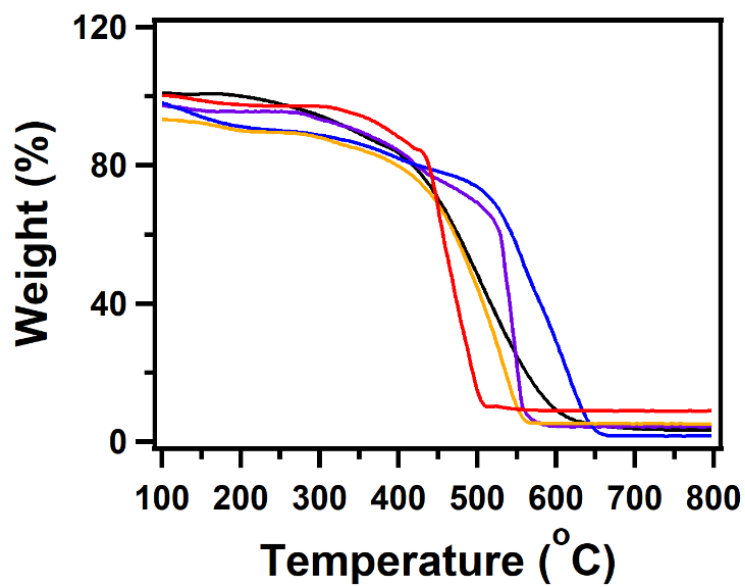


Figure S29. TGA curve of TFPPer-COCHDA COF under nitrogen atmosphere.

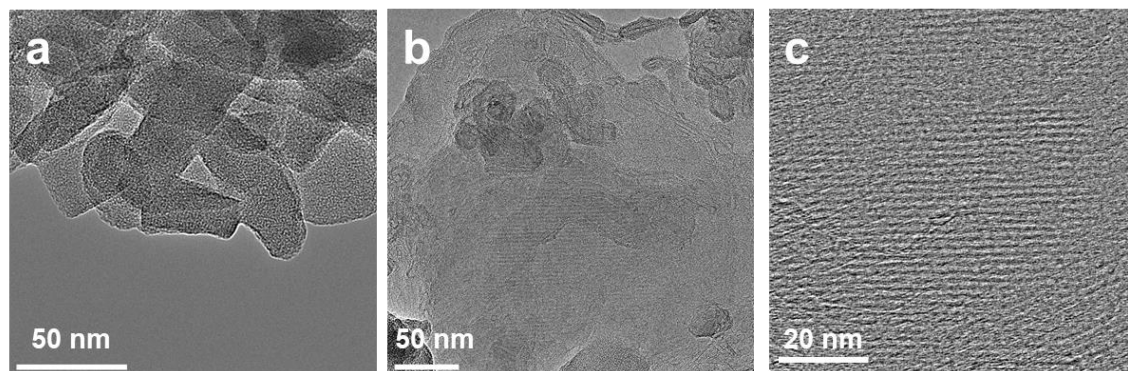


Figure S30. HR-TEM images of ETTA-CHDA COF with kgm topology. (a)(b) Low-magnification images of ETTA-CHDA COF, showing its morphology. (c) TEM image showing a periodic structure.

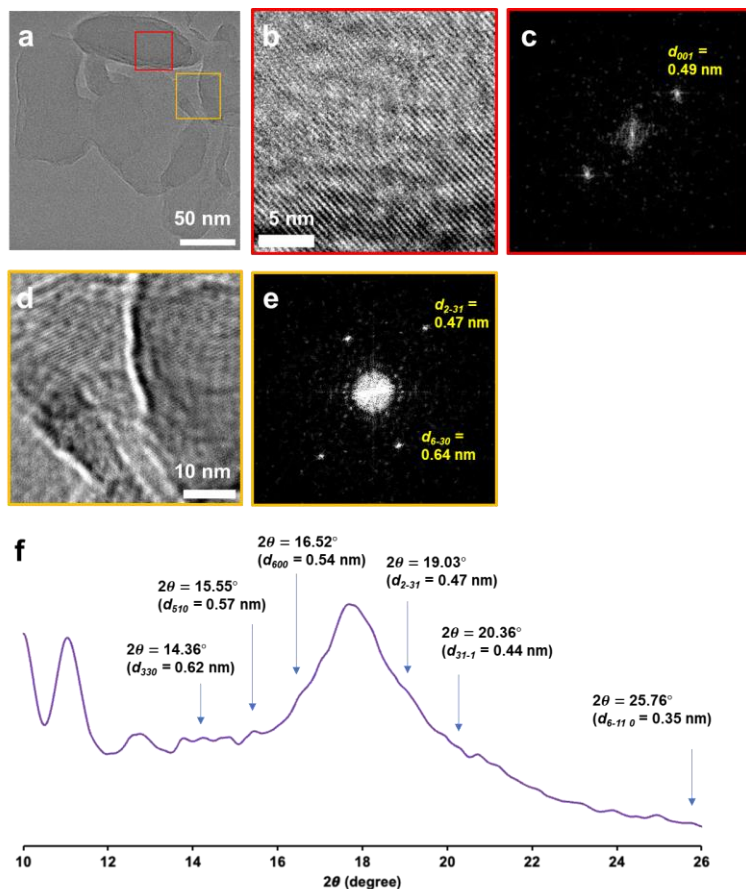


Figure S31. HR-TEM and FFT images of ETTA-CHDA COF. (a) TEM images of ETTA-CHDA COF. (b) Magnified TEM image of the area inside a red square in (a). (c) FFT image of (b). (d) Magnified TEM image of the area inside an orange square in (a). (e) FFT image of (d). (f) Magnified PXRD simulation spectra. Blue arrows indicate the diffraction observed in the TEM images, but not in experimental PXRD.

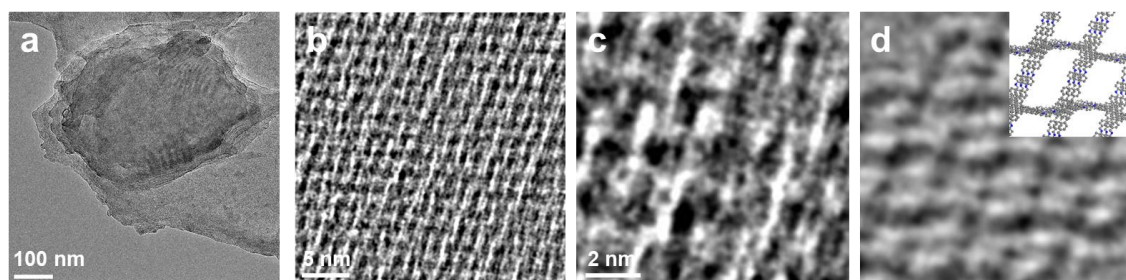


Figure S32. HR-TEM images of TFP Perry-CHDA COF with sql topology. (a) Low-magnification images of TFP Perry-CHDA COF. (b) TEM image showing a periodic structure. (c) Magnified TEM image. (d) An image simulated from molecular model. Molecular model is partially overlaid.

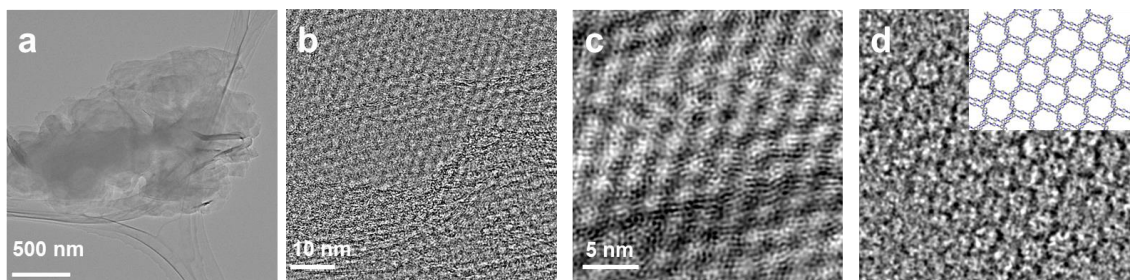


Figure S33. HR-TEM images of TFB-CHDA COF with hcb topology. (a) Low-magnification images of TFB-CHDA COF. (b) TEM image showing a periodic structure. (c) Magnified TEM image. (d) An image simulated from molecular model. Molecular model is partially overlaid.

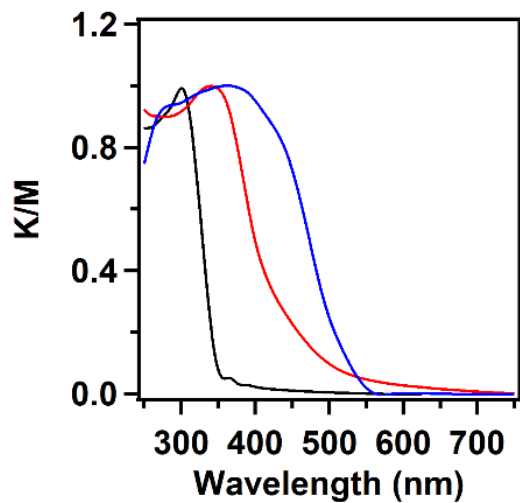


Figure S34. The UV-vis diffuse reflectance spectra (DRS) of TFB (black curve), TFPB (blue curve) and ETTA (red curve) monomers.

Section D: Fluorescent Sensor Experiments

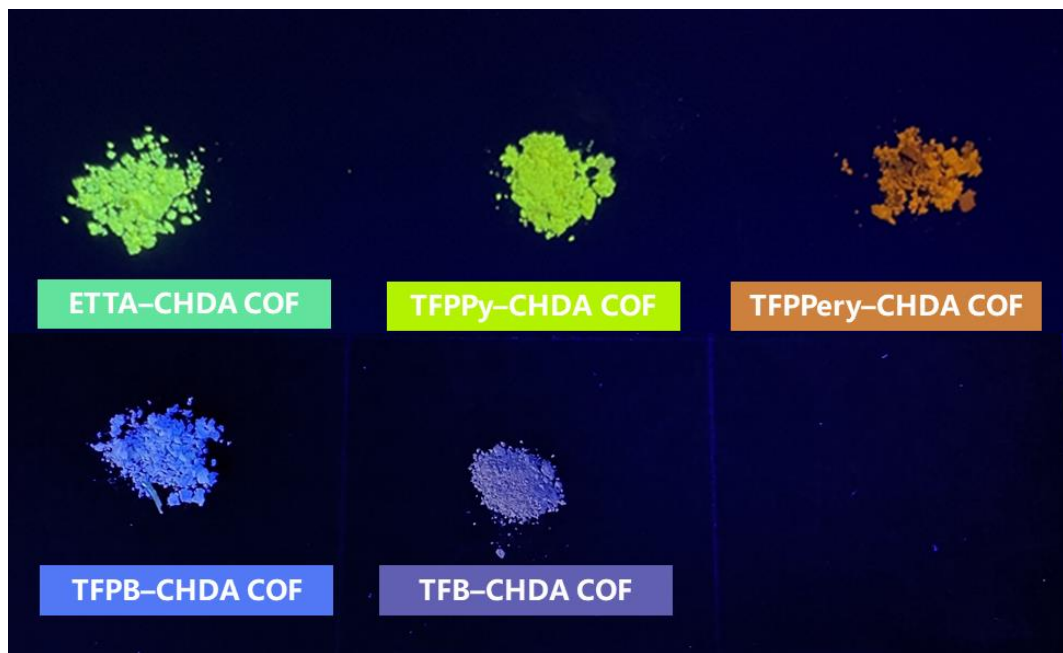


Figure S35. The photoluminescent images of CHDA-based COFs powders under UV-illuminant of 365 nm.

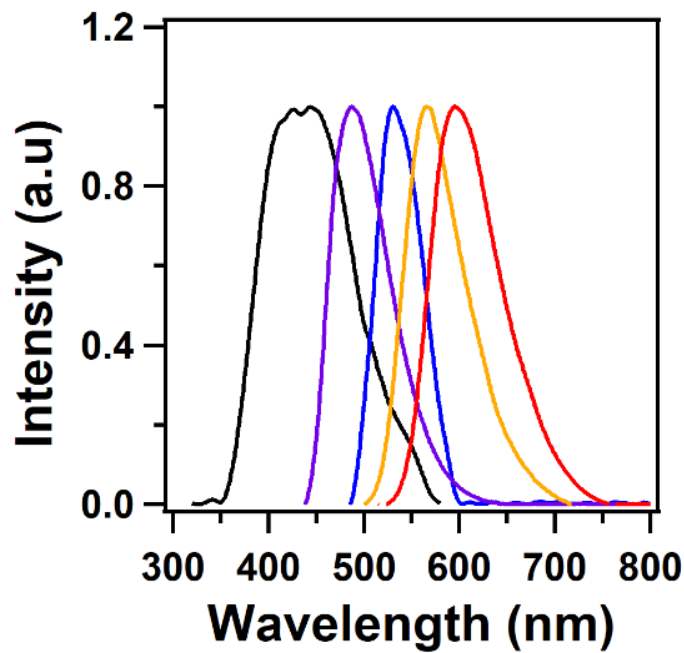


Figure S36. PL spectra of TFB (black curve), TFPB (purple curve), ETTA (blue curve), TFPPy (orange curve) and TFPPer (red curve) in the solid-state.

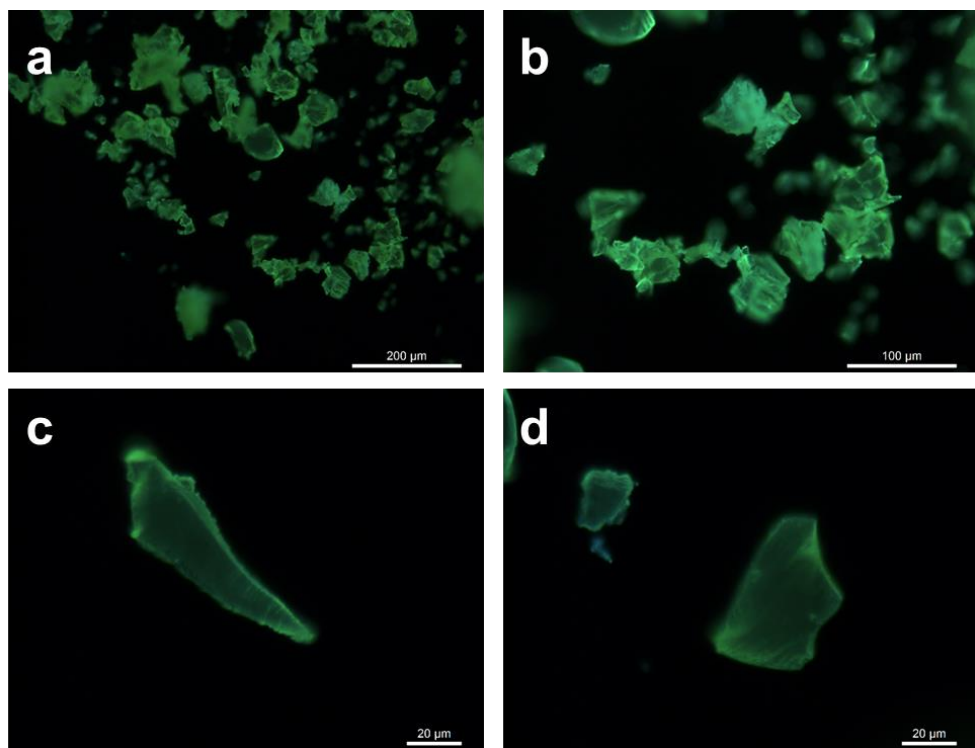


Figure S37. The fluorescence microscope images of the representative ETTA-CHDA COF with the highest PLQY and bright green luminescence across the particles.

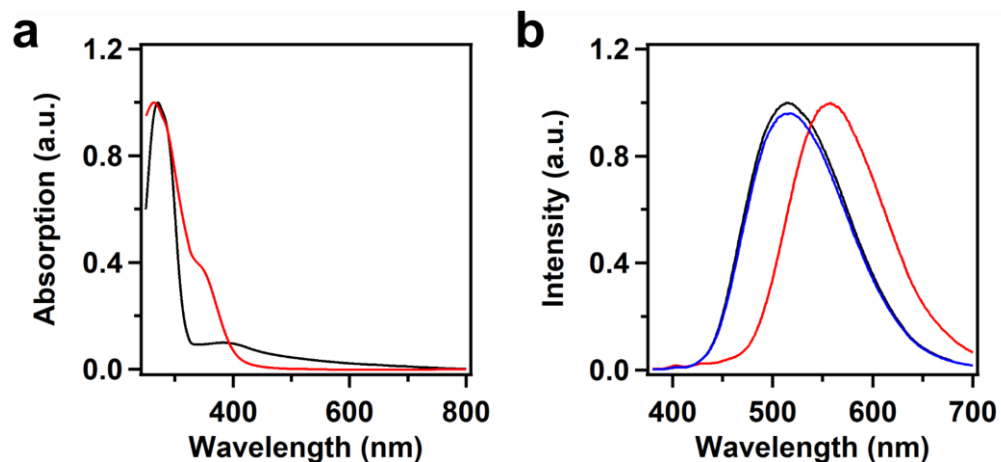


Figure S38. (a) Fluorescent emission and (b) UV-vis absorption spectra of pristine (black curve), acidic state (red curve) and neutralized states with TEA (blue curve) of ETTA-CHDA-COF in THF solutions. Black and blue curves were normalized with the same ratio of the initial luminescent intensity.

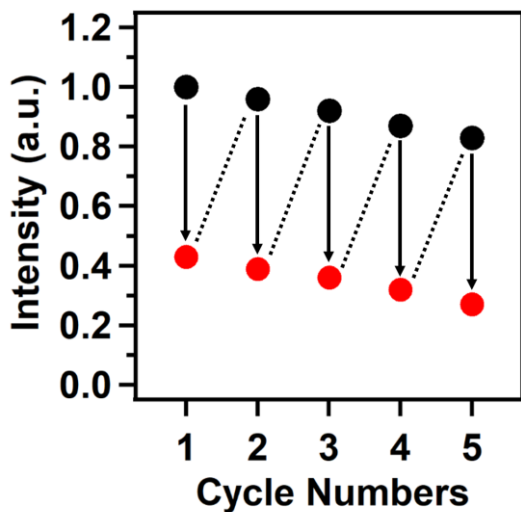


Figure S39. Recycling tests of ETTA-CHDA-COF after cycles of acid sensing, neutralization, and collection, based on the PL intensity in THF. From the initial intensity normalized to 1.0, addition of TFA solution (0.06 M in THF, 250 μ L) resulted in the partial PL quenching (red dots). After neutralization with TEA solution (0.03 M in THF, 250 μ L) and collection by filtration, recycled ETTA-CHDA-COF, re-dispersed in THF, displayed recovered PL intensity (black dot). This cycle was repeated to demonstrate the high recyclability, while the gradual decrease in the PL intensity could be due to the loss of COF powders during the filtration and re-dispersion.

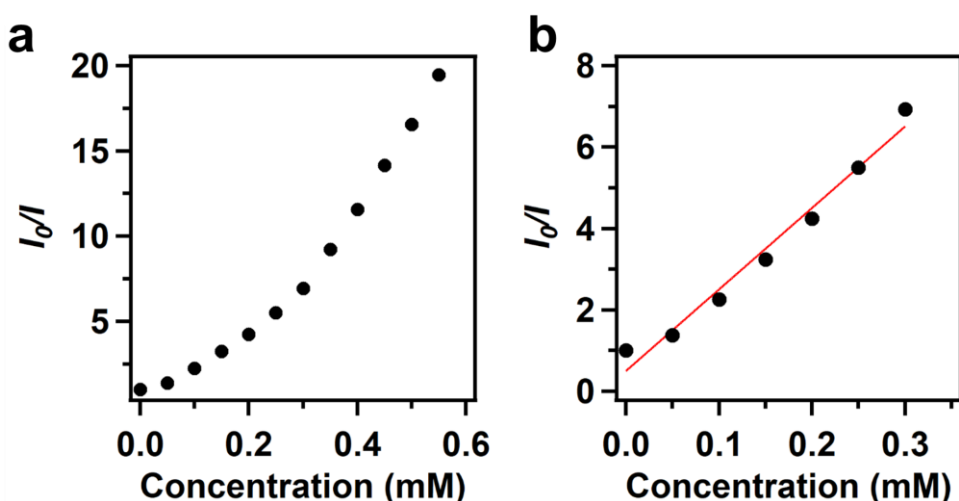


Figure S40. (a) Stern-Völmer plot of ETTA-CHDA COF THF solution ($c = 50 \mu\text{g mL}^{-1}$) upon titration with Fe^{3+} solution (0.015 M in THF) at room temperature ($\lambda_{\text{ex}} = 360 \text{ nm}$). (b) Stern-Volmer plots and K_a constant at lower concentration region for the Fe^{3+}

detection ($K_{\text{sv}} = 2.00 \times 10^4 \text{ M}^{-1}$).

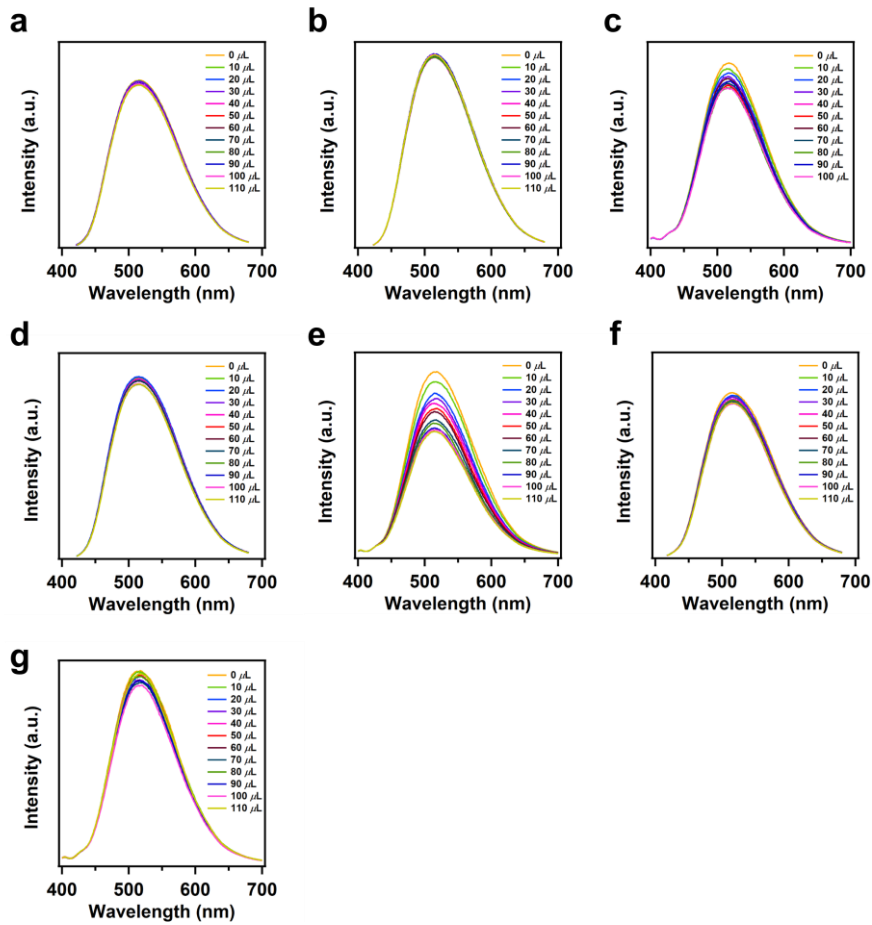


Figure S41. (a) Fluorescence emission spectra of ETTA-CHDA COF THF solutions ($c = 50 \mu\text{g mL}^{-1}$) upon successive addition of (a) Na^+ , (b) Mg^{2+} , (c) Cu^{2+} , (d) Zn^{2+} , (e) Ni^{2+} , (f) Co^{2+} , (g) Fe^{2+} solutions (0.015 M in THF) at room temperature ($\lambda_{\text{ex}} = 360 \text{ nm}$).

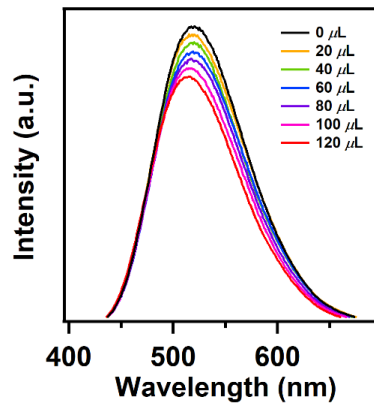


Figure S42. Emission spectra of ETTA-CHDA COF aqueous solution ($c = 50 \mu\text{g mL}^{-1}$) upon titration with Fe^{3+} solution (0.03 M in water) at room temperature ($\lambda_{\text{ex}} =$

360 nm).

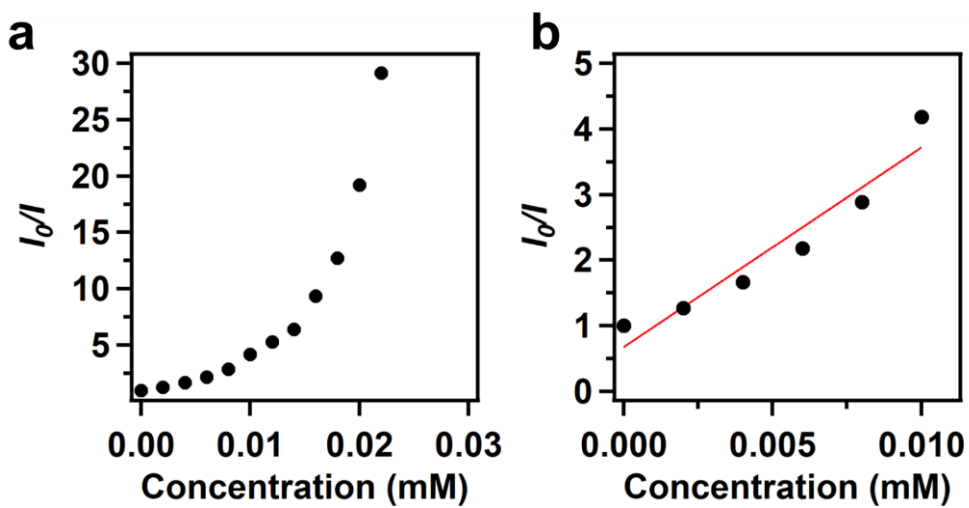


Figure S43. (a) Stern-Völmer plot of ETTA-CHDA COF in THF solution ($c = 50 \mu\text{g mL}^{-1}$) upon successive addition of PA solution ($6 \times 10^{-4} \text{ M}$ in THF) at room temperature ($\lambda_{\text{ex}} = 360 \text{ nm}$). (b) Stern-Volmer plots and K_a constant at lower concentration region for the PA detection ($K_{\text{sv}} = 3.04 \times 10^5 \text{ M}^{-1}$).

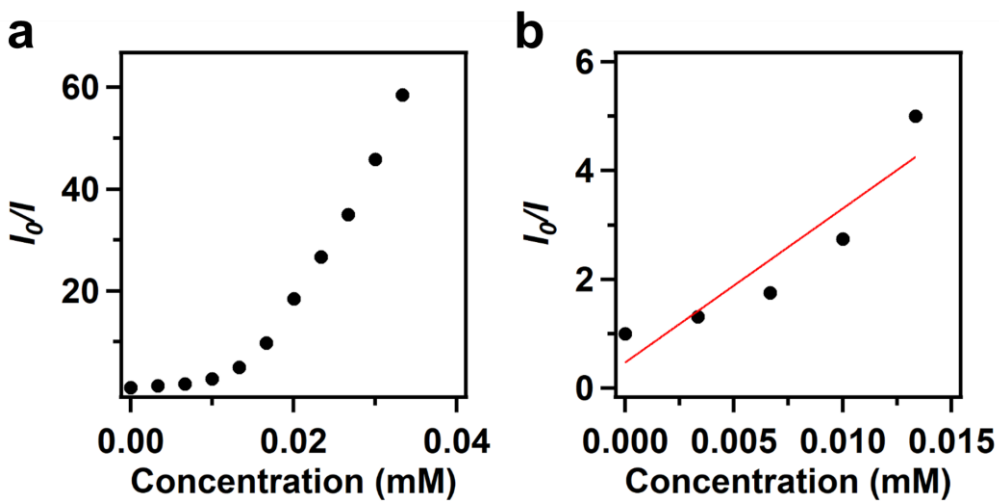


Figure S44. (a) Stern-Völmer plot of ETTA-CHDA COF in THF solution ($c = 50 \mu\text{g mL}^{-1}$) upon successive addition of PGA solution ($1 \times 10^{-3} \text{ M}$ in THF) at room temperature ($\lambda_{\text{ex}} = 360 \text{ nm}$). (b) Stern-Volmer plots and K_a constant at lower concentration region for the PGA sensing ($K_{\text{sv}} = 2.83 \times 10^5 \text{ M}^{-1}$).

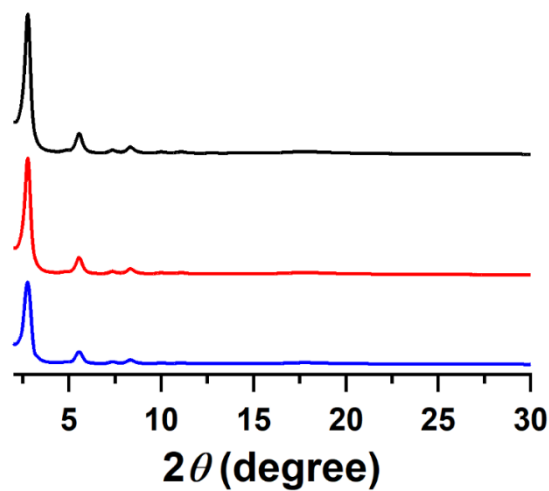


Figure S45. PXRD pattern of ETTA-CHDA COF after sensing for Fe^{3+} (blue curve), PA (red curve) and PGA (black curve).

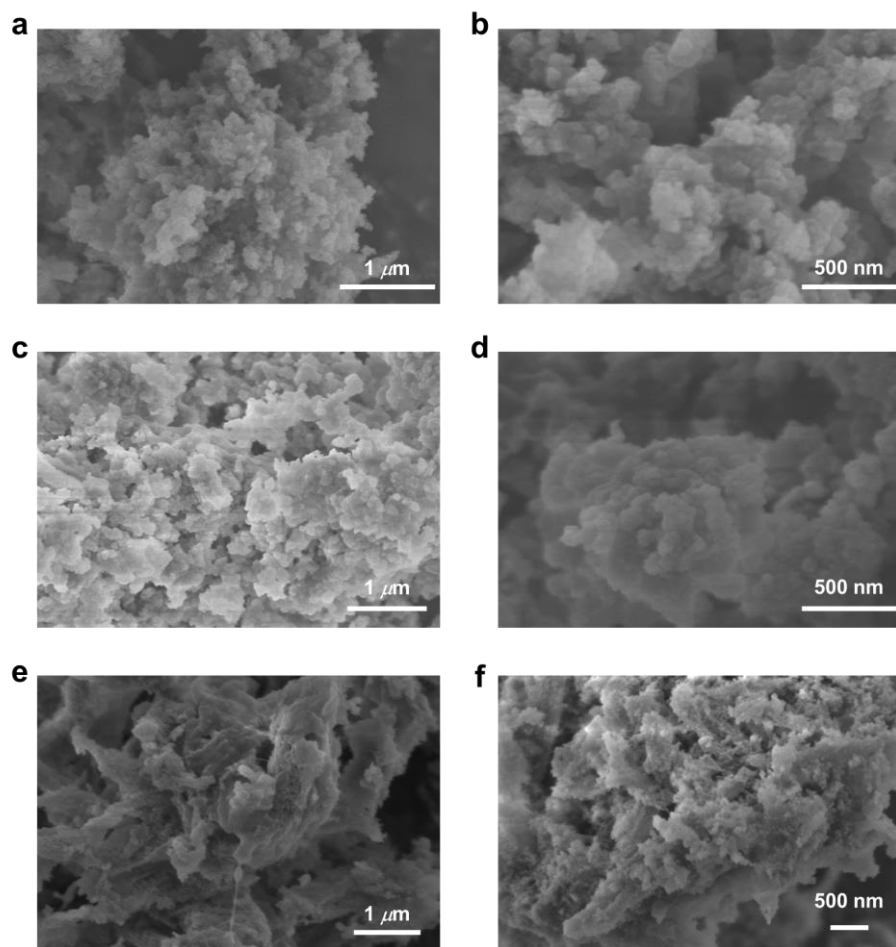


Figure S46. SEM images of ETTA-CHDA COF after sensing for Fe^{3+} (a and b), PA (c and d) and PGA (e and f).

Table S1. Solvothermal conditions and corresponding results of crystallinity for TFB-CHDA COF, TFPB-CHDA COF, ETTA-CHDA COF, TFPPy-CHDA COF and TFPPery-CHDA COF.

COFs	Ratio of Solvents (v/v, V _{total} = 3 mL)	Catalyst (c/amount)	Temperature (°C)	Time (h)	Degree of Crystallinity
TFB-CHDA COF	DMAc	HAc (6 M/500 μL)	120	72	None
	DMAc	HAc (6 M/100 μL)	120	72	Weak
	n-BuOH	HAc (6 M/50 μL)	120	72	Weak
	DMAc/1,4-Dioxane (1/1)	HAc (6 M/50 μL)	120	72	Weak
	DMAc/1,4-Dioxane (4/1)	HAc (6 M/50 μL)	120	72	Strong
	DMAc/1,4-Dioxane (4/1)	HAc (6 M/300 μL)	120	72	Weak
	DMAc/1,4-Dioxane (8/1)	HAc (6 M/50 μL)	120	72	Weak
	ODCB/n-BuOH (1/1)	HAc (6 M/50 μL)	120	72	None
TFPB-CHDA COF	n-BuOH	HAc (6 M/50 μL)	120	72	Strong
	DMAc/1,4-Dioxane (4/1)	HAc (6 M/100 μL)	120	72	None
	DMAc/ODCB	HAc (6 M/50 μL)	120	72	None
	ODCB/n-BuOH (1/1)	HAc (6 M/50 μL)	120	72	Weak
	ODCB/n-BuOH (4/1)	HAc (6 M/50 μL)	120	72	Weak
ETTA-CHDA COF	n-BuOH	None	80	72	None
	n-BuOH	HAc (6 M/50 μL)	80	72	Weak
	n-BuOH	HAc (6 M/300 μL)	80	72	Weak
	Mesitylene/1,4-Dioxane (1/1)	None	120	72	Weak
	ODCB/n-BuOH (1/1)	None	120	72	None
	ODCB/n-BuOH (1/1)	HAc (6 M/300 μL)	120	72	None

	DMAc/Dioxane (1/1)	None	120	72	None
	DMAc/1,4-Dioxane (4/1)	HAc (6 M/100 μ L)	90	72	Weak
	DMAc/1,4-Dioxane (4/1)	HAc (6 M/60 μ L)	90	72	Strong
TFPPy-CHDA COF	Dioaxne	HAc (6 M/200 μ L)	120	72	None
	DMAc	HAc (6 M/200 μ L)	120	72	Weak
	DMAc/1,4-Dioxane (1/1)	HAc (6 M/50 μ L)	120	96	Weak
	DMAc/1,4-Dioxane (9/1)	HAc (6 M/100 μ L)	120	72	None
	DMAc/1,4-Dioxane (9/1)	HAc (6 M/100 μ L)	90	72	Weak
	DMAc/1,4-Dioxane (9/1)	HAc (6 M/60 μ L)	120	72	Weak
	1,4-Dioxane / <i>n</i> -BuOH (4/1)	HAc (6 M/50 μ L)	120	96	Weak
	1,4-Dioxane / <i>n</i> -BuOH (1/4)	HAc (3 M/50 μ L)	120	72	Strong
	1,4-Dioxane / <i>n</i> -BuOH (1/4)	HAc (6 M/50 μ L)	120	96	Weak
TFPPery- CHDA COF	<i>n</i> -BuOH	HAc (6 M/100 μ L)	120	72	Weak
	1,4-Dioxane	HAc (6 M/200 μ L)	120	72	None
	DMAc/1,4-Dioxane (4/1)	HAc (6 M/400 μ L)	120	72	Weak
	DMAc/1,4-Dioxane (4/1)	HAc (6 M/200 μ L)	120	72	Strong
	DMAc/1,4-Dioxane (4/1)	HAc (6 M/100 μ L)	90	72	Weak
	DMAc/1,4-Dioxane (4/1)	None	120	72	Weak
	DMAc/1,4-Dioxane (9/1)	HAc (6 M/200 μ L)	120	72	Weak
	DMAc/1,4-Dioxane (4/1)	HAc (6 M/50 μ L)	150	72	Weak
	DMAc/1,4-Dioxane (9/1)	HAc (6 M/100 μ L)	120	72	Strong
	Meistylene/1,4-Dioxane (1/1)	HAc (6 M/100 μ L)	120	72	None
	Meistylene/1,4-Dioxane (4/1)	HAc (6 M/100 μ L)	120	72	Weak

Table S2. Summary of the full-width at half-maximum (FWHM) of the first intense peaks in PXRD patterns of all the cyclohexane and phenylene-linked COFs.

	First Intense Peak Position (degree)	FWHM (degree)
TFB-CHDA-COF	4.09	0.25
TFPB-CHDA-COF	2.84	0.41
ETTA-CHDA-COF	2.77	0.45
TFPPy-CHDA-COF	4.10	0.68
TFPPery-CHDA-COF	4.22	0.43
TFPPery-PDA-COF	2.05	0.71

Table S3. Atomistic coordinates for the refined unit cell parameters for TFB-CHDA COF via Pawley refinement. Space group: $P1$; $a = b = 24.4657 \text{ \AA}$, $c = 7.0184 \text{ \AA}$, $\alpha = 90.0000^\circ$, $\beta = 90.0000^\circ$, and $\gamma = 120.1647^\circ$. Pawley-refined PXRD profile confirmed the correctness of the peak assignment as evident by a small difference with R_{wp} and R_p values of 0.75% and 1.56%, respectively.

H1	0.4453	0.4993	0.1717
H2	0.6198	0.6849	0.7664
H3	0.4937	0.5688	0.0318
H4	0.6686	0.7544	0.6295
H5	0.3450	0.4078	0.7413
H6	0.5177	0.5914	0.3528
H7	0.3537	0.4003	0.9914
H8	0.5318	0.5883	0.6002
H9	0.3945	0.6991	0.9443
H10	0.5747	0.8848	0.4688
H11	0.2855	0.7718	0.9053
H12	0.4730	0.9648	0.4217
H13	0.3871	0.8838	0.7828
H14	0.5849	0.0730	0.2611
H15	0.3814	0.9098	0.2090
H16	0.5705	0.0985	0.6782
H17	0.3204	0.8890	0.0363
H18	0.5109	0.0779	0.4986
H19	0.4970	0.9087	0.8461
H20	0.6915	0.0981	0.3518
H21	0.4900	0.9220	0.0896
H22	0.6785	0.1117	0.5937
H23	0.2023	0.6611	0.9660
H24	0.3847	0.8543	0.4647
H25	0.1280	0.4794	0.0115
H26	0.3046	0.6715	0.5252
H27	0.9905	0.4645	0.6914
H28	0.1593	0.6600	0.2396
H29	0.9767	0.5425	0.8829
H30	0.1593	0.7440	0.4650
H31	0.6537	0.4048	0.9400
H32	0.8278	0.5929	0.4935
H33	0.4712	0.3017	0.0033
H34	0.6468	0.4854	0.5572
H35	0.4576	0.3978	0.1068

H36	0.6357	0.5824	0.7003
H37	0.4001	0.3457	0.8067
H38	0.5737	0.5304	0.4124
H39	0.4493	0.4159	0.6728
H40	0.6218	0.5993	0.2699
H41	0.5366	0.5119	0.8439
H42	0.7141	0.6989	0.4456
H43	0.5496	0.5075	0.0914
H44	0.7237	0.6923	0.6958
H45	0.4938	0.2150	0.9684
H46	0.6726	0.4001	0.4963
H47	0.5954	0.1347	0.0120
H48	0.7806	0.3270	0.5430
H49	0.3839	0.9909	0.8644
H50	0.5766	0.1813	0.3401
H51	0.6839	0.2454	0.9740
H52	0.8645	0.4376	0.4745
H53	0.7640	0.4285	0.9172
H54	0.9390	0.6196	0.4308
H55	0.8723	0.4462	0.7900
H56	0.0503	0.6415	0.3338
H57	0.9083	0.4435	0.2015
H58	0.0809	0.6380	0.7598
H59	0.8817	0.4945	0.1013
H60	0.0594	0.6907	0.6510
H61	0.8946	0.3590	0.7397
H62	0.0697	0.5486	0.3109
H63	0.9112	0.3586	0.9874
H64	0.0916	0.5584	0.5532
C1	0.0181	0.4848	0.9749
C2	0.1977	0.6818	0.5267
H65	0.0163	0.4587	0.1069
H66	0.1966	0.6529	0.6475
H67	0.0125	0.4130	0.8045
H68	0.1860	0.6079	0.3305
H69	0.9988	0.5526	0.1247
H70	0.1778	0.7422	0.7105
C3	0.4741	0.0282	0.0181
C4	0.6642	0.2169	0.5044
C5	0.4987	0.9984	0.9008
C6	0.6917	0.1881	0.3943
H71	0.4866	0.0255	0.1672
H72	0.6758	0.2144	0.6557

H73	0.5510	0.0239	0.9123
H74	0.7437	0.2144	0.4163
H75	0.4858	0.0013	0.7517
H76	0.6835	0.1918	0.2408
H77	0.3797	0.0066	0.1111
H78	0.5685	0.1941	0.5828
N1	0.3640	0.5180	0.9321
N2	0.5404	0.7044	0.5119
C7	0.2563	0.5563	0.9509
C8	0.4335	0.7455	0.4925
C9	0.3733	0.5767	0.9201
C10	0.5499	0.7624	0.4785
C11	0.4114	0.4967	0.8813
C12	0.5875	0.6818	0.4727
C13	0.4659	0.5164	0.0280
C14	0.6411	0.7020	0.6233
C15	0.3801	0.4233	0.8587
C16	0.5553	0.6085	0.4619
C17	0.3233	0.5988	0.9452
C18	0.5009	0.7860	0.4864
N3	0.3798	0.8129	0.9792
N4	0.5690	0.0012	0.4648
C19	0.3444	0.6657	0.9518
C20	0.5242	0.8530	0.4750
C21	0.3226	0.7625	0.9490
C22	0.5094	0.9530	0.4497
C23	0.4009	0.8819	0.9320
C24	0.5935	0.0709	0.4144
C25	0.3724	0.9142	0.0569
C26	0.5625	0.1029	0.5266
C27	0.4740	0.9261	0.9459
C28	0.6663	0.1154	0.4434
C29	0.3019	0.6902	0.9612
C30	0.4841	0.8799	0.4679
N5	0.0877	0.5333	0.9353
N6	0.2671	0.7299	0.4826
C31	0.2355	0.6441	0.9638
C32	0.4166	0.8359	0.4703
C33	0.1379	0.5262	0.9691
C34	0.3161	0.7196	0.4954
C35	0.9872	0.4396	0.8275
C36	0.1608	0.6338	0.3664
C37	0.9771	0.5166	0.0124

C38	0.1566	0.7122	0.5824
C39	0.2105	0.5771	0.9573
C40	0.3894	0.7686	0.4837
N7	0.5278	0.3954	0.9280
N8	0.7037	0.5814	0.5083
C41	0.6352	0.3544	0.9478
C42	0.8109	0.5427	0.4892
C43	0.5186	0.3374	0.9612
C44	0.6941	0.5226	0.5204
C45	0.4805	0.4177	0.9671
C46	0.6566	0.6030	0.5595
C47	0.4274	0.3981	0.8150
C48	0.6016	0.5828	0.4144
C49	0.5125	0.4909	0.9809
C50	0.6882	0.6765	0.5794
C51	0.5677	0.3138	0.9528
C52	0.7440	0.5003	0.4949
N9	0.4992	0.0985	0.9729
N10	0.6873	0.2865	0.4575
C53	0.5443	0.2468	0.9629
C54	0.7227	0.4334	0.4884
C55	0.5590	0.1467	0.9869
C56	0.7442	0.3366	0.4935
C57	0.4001	0.9869	0.0091
C58	0.5908	0.1755	0.4844
C59	0.5845	0.2199	0.9696
C60	0.7651	0.4089	0.4792
N11	0.8018	0.3702	0.9577
N12	0.9794	0.5656	0.5032
C61	0.6520	0.2639	0.9684
C62	0.8316	0.4548	0.4765
C63	0.7527	0.3803	0.9458
C64	0.9292	0.5727	0.4714
C65	0.8712	0.4188	0.9145
C66	0.0487	0.6146	0.4633
C67	0.9070	0.4683	0.0714
C68	0.0840	0.6637	0.6257
C69	0.9142	0.3896	0.8673
C70	0.0907	0.5843	0.4242
C71	0.6793	0.3312	0.9563
C72	0.8566	0.5218	0.4827
H79	0.2395	0.5061	0.9465
H80	0.4149	0.6951	0.5015

H81	0.4206	0.6140	0.8839
H82	0.5973	0.7980	0.4364
H83	0.4328	0.5179	0.7415
H84	0.6100	0.7010	0.3320

Table S4. Atomistic coordinates for the refined unit cell parameters for TFPB-CHDA COF via Pawley refinement. Space group: $P1$; $a = 37.7014 \text{ \AA}$, $b = 36.1649 \text{ \AA}$, $c = 5.0332 \text{ \AA}$, $\alpha = 90.0000^\circ$, $\beta = 90.0000^\circ$, and $\gamma = 119.9003^\circ$. Pawley-refined PXRD profile confirmed the correctness of the peak assignment as evident by a small difference with R_{wp} and R_p values of 1.94% and 3.72%, respectively.

C1	0.3587	0.6402	0.8796
C2	0.3758	0.6845	0.8538
C3	0.4650	0.5687	0.9354
N4	0.4572	0.5350	0.7988
H5	0.4105	0.7063	0.8646
H6	0.4936	0.5850	1.0654
C7	0.3509	0.7027	0.8146
C8	0.3082	0.6759	0.8101
C9	0.4272	0.8826	0.5810
N10	0.4625	0.9098	0.6811
H11	0.2875	0.6902	0.7802
H12	0.4112	0.8938	0.4364
C13	0.2901	0.6314	0.8421
C14	0.3159	0.6140	0.8744
C15	0.1141	0.5209	0.8142
N16	0.0896	0.5363	0.7951
H17	0.3022	0.5780	0.8969
H18	0.1011	0.4849	0.8217
C19	0.4836	0.5162	0.7992
C20	0.4611	0.4729	0.6585
C21	0.5241	0.5458	0.6550
H22	0.4522	0.4775	0.4495
H23	0.4322	0.4505	0.7745
H24	0.5413	0.5771	0.7689
H25	0.5172	0.5525	0.4452
H26	0.4904	0.5113	1.0133
C27	0.4629	0.9776	0.7298
H28	0.4602	0.9725	0.9544
H29	0.4310	0.9637	0.6400
C30	0.9791	0.5117	0.7725
C31	0.9680	0.4906	0.4976
C32	0.9875	0.4626	0.4587
H33	0.9653	0.4859	0.9322
H34	0.9661	0.5341	0.7947
H35	0.9803	0.4485	0.2497

H36	0.9743	0.4356	0.6106
H37	0.9796	0.5164	0.3372
C38	0.5311	0.0459	0.7763
C39	0.4874	0.0258	0.6701
H40	0.4884	0.0309	0.4458
H41	0.4711	0.0417	0.7679
H42	0.5306	0.0436	1.0026
C43	0.0343	0.4886	0.4958
C44	0.0453	0.5095	0.7710
C45	0.0259	0.5376	0.8093
H46	0.0475	0.4665	0.4735
H47	0.0478	0.5144	0.3359
H48	0.0394	0.5647	0.6579
H49	0.0328	0.5517	1.0186
H50	0.0334	0.4837	0.9309
C51	0.4845	0.9550	0.6102
C52	0.5283	0.9750	0.7174
H53	0.5444	0.9589	0.6194
H54	0.5275	0.9700	0.9418
H55	0.4855	0.9583	0.3844
C56	0.6542	0.3584	0.4231
C57	0.6373	0.3144	0.4605
C58	0.5472	0.4291	0.3619
N59	0.5550	0.4630	0.4963
H60	0.6026	0.2925	0.4570
H61	0.5185	0.4125	0.2335
C62	0.6625	0.2966	0.5027
C63	0.7052	0.3235	0.4979
C64	0.5882	0.1186	0.7852
N65	0.5523	0.0905	0.6958
H66	0.7262	0.3095	0.5296
H67	0.6051	0.1084	0.9293
C68	0.7230	0.3677	0.4544
C69	0.6969	0.3848	0.4194
C70	0.8989	0.4788	0.4570
N71	0.9236	0.4637	0.4755
H72	0.7105	0.4205	0.3873
H73	0.9117	0.5148	0.4465
C74	0.5286	0.4818	0.4954
C75	0.5511	0.5251	0.6359
C76	0.4882	0.4522	0.6395
H77	0.5801	0.5472	0.5202
H78	0.5598	0.5206	0.8458

H79	0.4951	0.4453	0.8486
H80	0.4707	0.4209	0.5254
H81	0.5218	0.4866	0.2812
C82	0.5528	0.0232	0.6594
H83	0.5846	0.0373	0.7507
H84	0.5557	0.0281	0.4347
C85	0.3854	0.6212	0.9007
C86	0.4229	0.6426	1.0371
C87	0.4486	0.6251	1.0498
C88	0.4374	0.5862	0.9246
C89	0.3999	0.5647	0.7887
C90	0.3742	0.5820	0.7774
C91	0.1587	0.5495	0.8265
C92	0.1760	0.5939	0.8148
C93	0.2186	0.6204	0.8207
C94	0.2446	0.6032	0.8381
C95	0.2268	0.5585	0.8506
C96	0.1843	0.5320	0.8446
C97	0.3697	0.7492	0.7662
C98	0.3503	0.7650	0.6007
C99	0.3690	0.8086	0.5436
C100	0.4073	0.8371	0.6518
C101	0.4267	0.8217	0.8196
C102	0.4081	0.7781	0.8758
C103	0.5750	0.4117	0.3736
C104	0.6128	0.4339	0.5046
C105	0.6387	0.4168	0.5172
C106	0.6272	0.3772	0.4001
C107	0.5894	0.3551	0.2686
C108	0.5636	0.3724	0.2546
C109	0.7685	0.3961	0.4504
C110	0.7861	0.4407	0.4331
C111	0.8285	0.4674	0.4329
C112	0.8544	0.4501	0.4495
C113	0.8372	0.4057	0.4655
C114	0.7947	0.3790	0.4658
C115	0.6440	0.2504	0.5641
C116	0.6645	0.2360	0.7309
C117	0.6463	0.1929	0.7999
C118	0.6074	0.1635	0.7028
C119	0.5870	0.1776	0.5340
C120	0.6052	0.2207	0.4658
H121	0.4323	0.6744	1.1379

H122	0.4788	0.6426	1.1624
H123	0.3905	0.5329	0.6869
H124	0.3437	0.5643	0.6674
H125	0.1553	0.6084	0.8004
H126	0.2325	0.6566	0.8114
H127	0.2471	0.5435	0.8658
H128	0.1704	0.4958	0.8546
H129	0.3190	0.7419	0.5126
H130	0.3529	0.8210	0.4084
H131	0.4577	0.8447	0.9108
H132	0.4240	0.7657	1.0116
H133	0.6223	0.4661	0.6012
H134	0.6695	0.4351	0.6232
H135	0.5796	0.3228	0.1724
H136	0.5330	0.3543	0.1458
H137	0.7651	0.4549	0.4191
H138	0.8423	0.5035	0.4191
H139	0.8580	0.3913	0.4785
H140	0.7809	0.3430	0.4787
H141	0.6962	0.2598	0.8101
H142	0.6631	0.1816	0.9360
H143	0.5555	0.1539	0.4518
H144	0.5884	0.2321	0.3292

Table S5. Atomistic coordinates for the refined unit cell parameters for ETTA-CHDA COF via Pawley refinement. Space group: $P1$; $a = b = 38.0273 \text{ \AA}$, $c = 5.0243 \text{ \AA}$, $\alpha = 89.9399^\circ$, $\beta = 89.9455^\circ$, and $\gamma = 121.6771^\circ$. Pawley-refined PXRD profile confirmed the correctness of the peak assignment as evident by a small difference with R_{wp} and R_p values of 2.43% and 3.14%, respectively.

C1	0.4800	0.4848	0.4365
C2	0.4450	0.4927	0.4316
C3	0.4118	0.4694	0.2631
C4	0.3792	0.4765	0.2496
C5	0.3789	0.5065	0.4095
C6	0.4111	0.5289	0.5845
C7	0.4435	0.5216	0.5974
H8	0.4690	0.5396	0.7454
C9	0.4682	0.4411	0.4425
C10	0.4419	0.4158	0.6423
C11	0.4335	0.3759	0.6678
C12	0.4507	0.3604	0.4900
C13	0.4745	0.3845	0.2768
C14	0.4830	0.4246	0.2542
C15	0.3448	0.5149	0.3910
C16	0.4449	0.3190	0.5380
H17	0.4111	0.4444	0.1352
H18	0.3529	0.4579	0.1082
H19	0.4107	0.5531	0.7166
H20	0.4272	0.4279	0.7857
H21	0.4126	0.3558	0.8335
H22	0.4867	0.3713	0.1230
H23	0.5022	0.4439	0.0804
C24	0.7185	0.1968	0.6037
C25	0.7553	0.1987	0.4572
C26	0.7942	0.2387	0.5152
C27	0.7898	0.2751	0.4335
C28	0.7535	0.2737	0.5804
C29	0.7144	0.2337	0.5264
H30	0.7241	0.1979	0.8272
N31	0.8271	0.3120	0.4967
N32	0.6803	0.1601	0.5434
H33	0.7493	0.1960	0.2337
H34	0.7596	0.1726	0.5263
H35	0.8204	0.2396	0.3999

H36	0.8011	0.2410	0.7373
H37	0.7842	0.2739	0.2098
H38	0.7496	0.3001	0.5100
H39	0.7596	0.2766	0.8037
H40	0.6886	0.2331	0.6456
H41	0.7071	0.2322	0.3051
H42	0.3498	0.5442	0.2946
H43	0.4130	0.2919	0.5644
C44	0.5152	0.9952	0.4365
C45	0.5073	0.9524	0.4316
C46	0.5306	0.9423	0.2631
C47	0.5235	0.9027	0.2496
C48	0.4935	0.8724	0.4095
C49	0.4711	0.8822	0.5845
C50	0.4784	0.9219	0.5974
H51	0.4604	0.9294	0.7454
C52	0.5589	0.0271	0.4425
C53	0.5842	0.0261	0.6423
C54	0.6242	0.0577	0.6678
C55	0.6396	0.0903	0.4900
C56	0.6155	0.0899	0.2768
C57	0.5754	0.0584	0.2542
C58	0.4851	0.8299	0.3910
C59	0.6810	0.1260	0.5380
H60	0.5556	0.9668	0.1352
H61	0.5421	0.8950	0.1082
H62	0.4469	0.8576	0.7166
H63	0.5721	0.9993	0.7857
H64	0.6442	0.0569	0.8335
H65	0.6287	0.1154	0.1230
H66	0.5561	0.0583	0.0804
C67	0.8032	0.5217	0.6037
C68	0.8013	0.5565	0.4572
C69	0.7613	0.5555	0.5152
C70	0.7249	0.5146	0.4335
C71	0.7263	0.4798	0.5804
C72	0.7663	0.4807	0.5264
H73	0.8021	0.5262	0.8272
N74	0.6880	0.5151	0.4967
N75	0.8399	0.5202	0.5434
H76	0.8041	0.5533	0.2337
H77	0.8275	0.5870	0.5263
H78	0.7604	0.5809	0.3999

H79	0.7590	0.5601	0.7373
H80	0.7261	0.5104	0.2098
H81	0.7000	0.4495	0.5100
H82	0.7234	0.4829	0.8037
H83	0.7669	0.4555	0.6456
H84	0.7678	0.4749	0.3051
H85	0.4558	0.8056	0.2946
H86	0.7081	0.1212	0.5644
C87	0.0048	0.5200	0.4365
C88	0.0476	0.5550	0.4316
C89	0.0577	0.5883	0.2631
C90	0.0973	0.6208	0.2496
C91	0.1276	0.6211	0.4095
C92	0.1178	0.5890	0.5845
C93	0.0781	0.5565	0.5974
H94	0.0706	0.5310	0.7454
C95	0.9729	0.5318	0.4425
C96	0.9739	0.5581	0.6423
C97	0.9423	0.5665	0.6678
C98	0.9097	0.5493	0.4900
C99	0.9101	0.5255	0.2768
C100	0.9416	0.5170	0.2542
C101	0.1701	0.6552	0.3910
C102	0.8740	0.5551	0.5380
H103	0.0332	0.5889	0.1352
H104	0.1050	0.6471	0.1082
H105	0.1424	0.5893	0.7166
H106	0.0007	0.5728	0.7857
H107	0.9431	0.5874	0.8335
H108	0.8846	0.5133	0.1230
H109	0.9417	0.4978	0.0804
C110	0.4783	0.2815	0.6037
C111	0.4435	0.2447	0.4572
C112	0.4446	0.2058	0.5152
C113	0.4854	0.2102	0.4335
C114	0.5202	0.2465	0.5804
C115	0.5193	0.2856	0.5264
H116	0.4738	0.2759	0.8272
N117	0.4850	0.1729	0.4967
N118	0.4798	0.3197	0.5434
H119	0.4467	0.2508	0.2337
H120	0.4130	0.2405	0.5263
H121	0.4192	0.1796	0.3999

H122	0.4399	0.1989	0.7373
H123	0.4896	0.2158	0.2098
H124	0.5505	0.2505	0.5100
H125	0.5171	0.2404	0.8037
H126	0.5445	0.3114	0.6456
H127	0.5251	0.2929	0.3051
H128	0.1944	0.6502	0.2946
H129	0.8789	0.5870	0.5644
C130	0.5200	0.5152	0.4365
C131	0.5550	0.5073	0.4316
C132	0.5883	0.5306	0.2631
C133	0.6208	0.5235	0.2496
C134	0.6211	0.4935	0.4095
C135	0.5890	0.4711	0.5845
C136	0.5565	0.4784	0.5974
H137	0.5310	0.4604	0.7454
C138	0.5318	0.5589	0.4425
C139	0.5581	0.5842	0.6423
C140	0.5665	0.6242	0.6678
C141	0.5493	0.6396	0.4900
C142	0.5255	0.6155	0.2768
C143	0.5170	0.5754	0.2542
C144	0.6552	0.4851	0.3910
C145	0.5551	0.6810	0.5380
H146	0.5889	0.5556	0.1352
H147	0.6471	0.5421	0.1082
H148	0.5893	0.4469	0.7166
H149	0.5728	0.5721	0.7857
H150	0.5874	0.6442	0.8335
H151	0.5133	0.6287	0.1230
H152	0.4978	0.5561	0.0804
C153	0.2815	0.8032	0.6037
C154	0.2447	0.8013	0.4572
C155	0.2058	0.7613	0.5152
C156	0.2102	0.7249	0.4335
C157	0.2465	0.7263	0.5804
C158	0.2856	0.7663	0.5264
H159	0.2759	0.8021	0.8272
N160	0.1729	0.6880	0.4967
N161	0.3197	0.8399	0.5434
H162	0.2508	0.8041	0.2337
H163	0.2405	0.8275	0.5263
H164	0.1796	0.7604	0.3999

H165	0.1989	0.7590	0.7373
H166	0.2158	0.7261	0.2098
H167	0.2505	0.7000	0.5100
H168	0.2404	0.7234	0.8037
H169	0.3114	0.7669	0.6456
H170	0.2929	0.7678	0.3051
H171	0.6502	0.4558	0.2946
H172	0.5870	0.7081	0.5644
C173	0.4848	0.0048	0.4365
C174	0.4927	0.0476	0.4316
C175	0.4694	0.0577	0.2631
C176	0.4765	0.0973	0.2496
C177	0.5065	0.1276	0.4095
C178	0.5289	0.1178	0.5845
C179	0.5216	0.0781	0.5974
H180	0.5396	0.0706	0.7454
C181	0.4411	0.9729	0.4425
C182	0.4158	0.9739	0.6423
C183	0.3759	0.9423	0.6678
C184	0.3604	0.9097	0.4900
C185	0.3845	0.9101	0.2768
C186	0.4246	0.9416	0.2542
C187	0.5149	0.1701	0.3910
C188	0.3190	0.8740	0.5380
H189	0.4444	0.0332	0.1352
H190	0.4579	0.1050	0.1082
H191	0.5531	0.1424	0.7166
H192	0.4279	0.0007	0.7857
H193	0.3558	0.9431	0.8335
H194	0.3713	0.8846	0.1230
H195	0.4439	0.9417	0.0804
C196	0.1968	0.4783	0.6037
C197	0.1987	0.4435	0.4572
C198	0.2387	0.4446	0.5152
C199	0.2751	0.4854	0.4335
C200	0.2737	0.5202	0.5804
C201	0.2337	0.5193	0.5264
H202	0.1979	0.4738	0.8272
N203	0.3120	0.4850	0.4967
N204	0.1601	0.4798	0.5434
H205	0.1960	0.4467	0.2337
H206	0.1726	0.4130	0.5263
H207	0.2396	0.4192	0.3999

H208	0.2410	0.4399	0.7373
H209	0.2739	0.4896	0.2098
H210	0.3001	0.5505	0.5100
H211	0.2766	0.5171	0.8037
H212	0.2331	0.5445	0.6456
H213	0.2322	0.5251	0.3051
H214	0.5442	0.1944	0.2946
H215	0.2919	0.8789	0.5644
C216	0.9952	0.4800	0.4365
C217	0.9524	0.4450	0.4316
C218	0.9423	0.4118	0.2631
C219	0.9027	0.3792	0.2496
C220	0.8724	0.3789	0.4095
C221	0.8822	0.4111	0.5845
C222	0.9219	0.4435	0.5974
H223	0.9294	0.4690	0.7454
C224	0.0271	0.4682	0.4425
C225	0.0261	0.4419	0.6423
C226	0.0577	0.4335	0.6678
C227	0.0903	0.4507	0.4900
C228	0.0899	0.4745	0.2768
C229	0.0584	0.4830	0.2542
C230	0.8299	0.3448	0.3910
C231	0.1260	0.4449	0.5380
H232	0.9668	0.4111	0.1352
H233	0.8950	0.3529	0.1082
H234	0.8576	0.4107	0.7166
H235	0.9993	0.4272	0.7857
H236	0.0569	0.4126	0.8335
H237	0.1154	0.4867	0.1230
H238	0.0583	0.5022	0.0804
C239	0.5217	0.7185	0.6037
C240	0.5565	0.7553	0.4572
C241	0.5555	0.7942	0.5152
C242	0.5146	0.7898	0.4335
C243	0.4798	0.7535	0.5804
C244	0.4807	0.7144	0.5264
H245	0.5262	0.7241	0.8272
N246	0.5151	0.8271	0.4967
N247	0.5202	0.6803	0.5434
H248	0.5533	0.7493	0.2337
H249	0.5870	0.7596	0.5263
H250	0.5809	0.8204	0.3999

H251	0.5601	0.8011	0.7373
H252	0.5104	0.7842	0.2098
H253	0.4495	0.7496	0.5100
H254	0.4829	0.7596	0.8037
H255	0.4555	0.6886	0.6456
H256	0.4749	0.7071	0.3051
H257	0.8056	0.3498	0.2946
H258	0.1212	0.4130	0.5644

Table S6. Atomistic coordinates for the refined unit cell parameters for TFPPy-CHDA COF via Pawley refinement. Space group: $P1$; $a = 29.8609 \text{ \AA}$, $b = 37.9624 \text{ \AA}$, $c = 4.9700 \text{ \AA}$, $\alpha = 60.2677^\circ$, $\beta = 90.0467^\circ$, and $\gamma = 91.3290^\circ$. Pawley-refined PXRD profile confirmed the correctness of the peak assignment as evident by a small difference with R_{wp} and R_{p} values of 0.65% and 0.99%, respectively.

C1	0.0349	0.9300	0.4609
C2	0.0342	0.9692	0.4319
C3	0.0686	0.9975	0.2790
C4	0.9157	0.8948	0.7132
C5	0.9159	0.8523	0.8757
C6	0.8783	0.8303	0.8746
C7	0.8395	0.8505	0.7150
C8	0.8382	0.8928	0.5689
C9	0.8760	0.9148	0.5649
C10	0.1930	0.8493	0.3607
C11	0.7720	0.7699	0.6773
C12	0.7543	0.7914	0.3449
C13	0.7168	0.7666	0.3086
N14	0.6985	0.7029	0.3596
H15	0.6739	0.3289	0.0773
H16	0.4028	0.5134	0.8813
H17	0.5582	0.6620	0.0401
H18	0.6276	0.7002	0.0494
H19	0.6958	0.5849	0.6309
H20	0.6258	0.5466	0.6400
H21	0.7828	0.7955	0.1791
H22	0.7048	0.7827	0.0587
C23	0.5323	0.4308	0.3932
C24	0.5349	0.4690	0.3803
C25	0.5716	0.4953	0.2451
C26	0.4127	0.3992	0.6546
C27	0.4117	0.3567	0.8286
C28	0.3728	0.3354	0.8397
C29	0.3343	0.3562	0.6800
C30	0.3345	0.3986	0.5210
C31	0.3735	0.4199	0.5050
C32	0.6731	0.3349	0.2808
C33	0.2643	0.2758	0.6593
C34	0.2467	0.2971	0.3266
C35	0.2090	0.2723	0.2922

N36	0.1906	0.2084	0.3479
H37	0.2275	0.8636	0.3382
H38	0.8997	0.0080	0.9509
H39	0.0487	0.1629	0.0822
H40	0.1174	0.2033	0.0665
H41	0.1909	0.0903	0.6256
H42	0.1216	0.0499	0.6606
H43	0.2752	0.3008	0.1616
H44	0.1970	0.2882	0.0422
C45	0.9579	0.9184	0.6615
C46	0.9600	0.9545	0.6785
C47	0.9260	0.9648	0.8221
C48	0.0762	0.9118	0.4096
C49	0.0735	0.8864	0.2782
C50	0.1111	0.8653	0.2677
C51	0.1527	0.8706	0.3753
C52	0.1559	0.8966	0.4986
C53	0.1179	0.9163	0.5221
C54	0.8010	0.8282	0.6879
C55	0.2263	0.7912	0.3676
C56	0.2561	0.7786	0.6524
C57	0.2950	0.7524	0.6569
N58	0.3145	0.6925	0.6493
H59	0.2602	0.3483	0.6272
H60	0.6050	0.5524	0.1434
H61	0.4624	0.6193	0.8596
H62	0.3959	0.6602	0.8583
H63	0.3129	0.6038	0.4406
H64	0.3804	0.5681	0.3944
H65	0.2350	0.7607	0.8705
H66	0.3157	0.7429	0.8745
C67	0.4558	0.4217	0.5971
C68	0.4601	0.4572	0.6183
C69	0.4269	0.4685	0.7602
C70	0.5709	0.4113	0.3255
C71	0.5634	0.3885	0.1759
C72	0.5967	0.3637	0.1638
C73	0.6388	0.3617	0.2941
C74	0.6473	0.3854	0.4338
C75	0.6137	0.4099	0.4494
C76	0.2948	0.3342	0.6628
C77	0.7361	0.2909	0.5066
C78	0.7680	0.2791	0.7785

C79	0.8040	0.2501	0.7881
N80	0.8178	0.1886	0.7881
H81	0.7661	0.8417	0.6479
H82	0.0985	0.0563	0.1547
H83	0.9621	0.1126	0.9604
H84	0.8979	0.1537	0.9859
H85	0.8083	0.0994	0.5857
H86	0.8736	0.0636	0.5108
H87	0.7480	0.2638	1.0035
H88	0.8258	0.2406	1.0010
C89	0.9623	0.0681	0.6571
C90	0.9621	0.0294	0.6767
C91	0.9274	0.0012	0.8252
C92	0.0805	0.1040	0.3820
C93	0.0801	0.1465	0.2121
C94	0.1181	0.1688	0.2016
C95	0.1573	0.1489	0.3570
C96	0.1586	0.1066	0.5120
C97	0.1204	0.0843	0.5279
C98	0.8114	0.1520	0.8087
C99	0.2254	0.2301	0.3790
C100	0.2428	0.2089	0.7121
C101	0.2806	0.2335	0.7466
N102	0.2995	0.2973	0.6890
H103	0.2762	0.6416	0.6880
H104	0.5994	0.4871	0.1296
H105	0.4426	0.3396	0.9616
H106	0.3722	0.3009	0.9788
H107	0.3026	0.4157	0.4042
H108	0.3736	0.4544	0.3692
H109	0.2558	0.1777	0.7731
H110	0.2925	0.2176	0.9967
C111	0.4665	0.5711	0.5842
C112	0.4655	0.5320	0.6139
C113	0.4298	0.5050	0.7607
C114	0.5872	0.6020	0.3510
C115	0.5885	0.6445	0.1813
C116	0.6269	0.6657	0.1845
C117	0.6647	0.6445	0.3535
C118	0.6644	0.6022	0.5071
C119	0.6258	0.5811	0.5089
C120	0.3107	0.6560	0.6646
C121	0.7334	0.7245	0.3922

C122	0.7511	0.7030	0.7245
C123	0.7886	0.7278	0.7605
N124	0.8067	0.7916	0.7101
H125	0.7762	0.1385	0.8442
H126	0.0962	0.9906	0.1540
H127	0.9470	0.8355	1.0095
H128	0.8789	0.7958	1.0035
H129	0.8060	0.9093	0.4526
H130	0.8747	0.9492	0.4400
H131	0.7644	0.6720	0.7821
H132	0.8007	0.7117	1.0102
C133	0.0384	0.0802	0.4414
C134	0.0359	0.0443	0.4234
C135	0.0697	0.0342	0.2773
C136	0.9224	0.0860	0.7282
C137	0.9281	0.1106	0.8651
C138	0.8923	0.1327	0.8863
C139	0.8495	0.1291	0.7856
C140	0.8431	0.1036	0.6600
C141	0.8793	0.0830	0.6248
C142	0.1961	0.1716	0.3736
C143	0.7836	0.2121	0.8002
C144	0.7511	0.2246	0.5287
C145	0.7148	0.2523	0.5337
N146	0.7040	0.3169	0.5071
H147	0.7382	0.6520	0.4259
H148	0.3970	0.4476	0.8775
H149	0.5297	0.3901	0.0625
H150	0.5897	0.3449	0.0469
H151	0.6818	0.3848	0.5355
H152	0.6214	0.4289	0.5640
H153	0.7347	0.1964	0.5457
H154	0.6910	0.2609	0.3317
C155	0.5441	0.5797	0.3986
C156	0.5406	0.5436	0.3830
C157	0.5746	0.5317	0.2494
C158	0.4259	0.5909	0.6267
C159	0.4293	0.6164	0.7572
C160	0.3923	0.6385	0.7628
C161	0.3506	0.6342	0.6515
C162	0.3467	0.6083	0.5272
C163	0.3841	0.5877	0.5080
C164	0.7036	0.6662	0.3831

C165	0.2781	0.7146	0.6531
C166	0.2485	0.7273	0.3675
C167	0.2095	0.7534	0.3630
N168	0.1897	0.8129	0.3737
H169	0.2310	0.1581	0.4083
H170	0.8966	0.9431	0.9387
H171	0.0404	0.8828	0.1791
H172	0.1080	0.8437	0.1712
H173	0.1896	0.9020	0.5806
H174	0.1211	0.9361	0.6344
H175	0.2347	0.6990	0.3702
H176	0.1889	0.7629	0.1450
C177	0.4990	0.4817	0.4999
C178	0.4922	0.4085	0.4940
H179	0.5092	0.6242	0.4779
C180	-0.0025	0.9806	0.5540
C181	-0.0041	0.9061	0.5650
H182	0.0018	0.1223	0.5454
C183	0.5017	0.5191	0.4988
C184	0.5065	0.5936	0.4869
H185	0.4885	0.3786	0.4935
C186	-0.0016	0.0182	0.5503
C187	0.0012	0.0922	0.5470
H188	-0.0055	0.8755	0.5730
H189	0.7436	0.7667	0.8417
H190	0.7408	0.8223	0.2868
H191	0.6877	0.7634	0.4680
H192	0.2362	0.2733	0.8231
H193	0.2335	0.3282	0.2661
H194	0.1800	0.2695	0.4508
H195	0.2468	0.8107	0.1494
H196	0.2703	0.8067	0.6487
H197	0.3172	0.7706	0.4449
H198	0.7561	0.3070	0.2816
H199	0.7851	0.3074	0.7547
H200	0.8259	0.2660	0.5721
H201	0.2538	0.2328	0.2161
H202	0.2144	0.2054	0.8766
H203	0.3095	0.2360	0.5886
H204	0.7616	0.7276	0.2275
H205	0.7227	0.6990	0.8910
H206	0.8176	0.7308	0.6008
H207	0.7644	0.1941	1.0269

H208	0.7704	0.2414	0.3013
H209	0.6952	0.2357	0.7602
H210	0.2574	0.6953	0.8706
H211	0.2694	0.7454	0.1491
H212	0.1875	0.7346	0.5746

Table S7. Atomistic coordinates for the refined unit cell parameters for TFPPerY-CHDA COF via Pawley refinement. Space group: $P1$; $a = 42.2975 \text{ \AA}$, $b = 24.4438 \text{ \AA}$, $c = 4.9193 \text{ \AA}$, $\alpha = 90.8229^\circ$, $\beta = 112.3108^\circ$, and $\gamma = 90.3355^\circ$. Pawley-refined PXRD profile confirmed the correctness of the peak assignment as evident by a small difference with R_{wp} and R_p values of 0.66% and 1.36%, respectively.

C1	0.9040	0.9343	0.6869
C2	0.9031	0.9000	0.9117
C3	0.8721	0.8882	0.9401
C4	0.8416	0.9112	0.7483
C5	0.8425	0.9470	0.5327
C6	0.8732	0.9583	0.5013
C7	0.1711	0.7563	1.1334
C8	0.7718	0.8341	0.8855
C9	0.7448	0.8772	0.8760
C10	0.7104	0.8500	0.8332
N11	0.6817	0.7801	0.9954
H12	0.7069	0.4031	0.1083
H13	0.5660	0.7056	0.4966
H14	0.6190	0.7600	0.6649
H15	0.6577	0.6674	1.4635
H16	0.6051	0.6124	1.2900
H17	0.7404	0.9056	0.6916
H18	0.6989	0.8300	0.6148
C19	0.4130	0.3506	-0.2109
C20	0.4092	0.3085	-0.0358
C21	0.3792	0.2774	-0.1297
C22	0.3526	0.2882	-0.3998
C23	0.3568	0.3295	-0.5775
C24	0.3867	0.3608	-0.4822
C25	0.6849	0.3897	-0.0794
C26	0.2803	0.1982	-0.3928
C27	0.2524	0.2403	-0.4124
C28	0.2181	0.2129	-0.4557
N29	0.1894	0.1469	-0.2617
H30	0.1894	0.7682	1.3491
H31	0.0667	0.1180	-0.4556
H32	0.1221	0.1424	-0.4728
H33	0.1730	0.0423	0.2799
H34	0.1190	0.0206	0.3123
H35	0.2487	0.2681	-0.5984

H36	0.2068	0.1919	-0.6719
C37	0.0766	0.8435	0.8054
C38	0.0821	0.8006	0.6373
C39	0.1126	0.7709	0.7447
C40	0.1378	0.7840	1.0211
C41	0.1318	0.8263	1.1902
C42	0.1015	0.8561	1.0817
C43	0.8080	0.8948	0.7458
C44	0.2133	0.6951	1.0837
C45	0.2396	0.7368	1.0653
C46	0.2752	0.7113	1.1398
N47	0.3069	0.6407	0.9974
H48	0.3003	0.2674	-0.7076
H49	0.4156	0.6598	0.8546
H50	0.3644	0.6719	0.9631
H51	0.3367	0.5038	0.7301
H52	0.3891	0.4894	0.6469
H53	0.2417	0.7716	1.2193
H54	0.2865	0.6990	1.3742
C55	0.5877	0.4359	-0.0610
C56	0.5890	0.4020	-0.2909
C57	0.6205	0.3875	-0.3043
C58	0.6511	0.4077	-0.0928
C59	0.6498	0.4429	0.1284
C60	0.6187	0.4566	0.1453
C61	0.3197	0.2590	-0.4935
C62	0.7220	0.3306	-0.2212
C63	0.7488	0.3744	-0.2054
C64	0.7834	0.3484	-0.1630
N65	0.8131	0.2789	-0.3257
H66	0.7857	0.9090	0.5665
H67	0.9289	0.2064	0.1823
H68	0.8759	0.2606	0.0109
H69	0.8388	0.1663	-0.7973
H70	0.8913	0.1118	-0.6215
H71	0.7527	0.4030	-0.0186
H72	0.7951	0.3291	0.0545
C73	0.0879	0.0674	-0.0692
C74	0.0896	0.1014	-0.2922
C75	0.1212	0.1149	-0.3048
C76	0.1516	0.0938	-0.0987
C77	0.1499	0.0582	0.1150
C78	0.1186	0.0453	0.1305

C79	0.8203	0.2457	-0.5022
C80	0.2225	0.1718	-0.2147
C81	0.2495	0.1287	-0.2045
C82	0.2840	0.1557	-0.1594
N83	0.3131	0.2257	-0.3184
H84	0.2918	0.5744	0.7107
H85	0.4290	0.3012	0.1777
H86	0.3762	0.2460	0.0119
H87	0.3367	0.3385	-0.7867
H88	0.3889	0.3941	-0.6156
H89	0.2402	0.1041	-0.4106
H90	0.3023	0.1239	-0.1697
C91	0.5816	0.6559	0.8844
C92	0.5857	0.6979	0.7104
C93	0.6158	0.7287	0.8058
C94	0.6423	0.7176	1.0765
C95	0.6377	0.6765	1.2536
C96	0.6076	0.6455	1.1568
C97	0.3127	0.5988	0.8584
C98	0.7144	0.8078	1.0683
C99	0.7424	0.7658	1.0889
C100	0.7766	0.7934	1.1292
N101	0.8047	0.8590	0.9262
H102	0.8014	0.2366	-0.7190
H103	0.9262	0.8819	1.0652
H104	0.8718	0.8605	1.1090
H105	0.8191	0.9643	0.3779
H106	0.8720	0.9832	0.3182
H107	0.7336	0.7399	0.8864
H108	0.7953	0.7618	1.1238
C109	0.9140	0.1560	-0.2104
C110	0.9096	0.1984	-0.0343
C111	0.8794	0.2290	-0.1314
C112	0.8534	0.2173	-0.4057
C113	0.8584	0.1758	-0.5846
C114	0.8884	0.1451	-0.4863
C115	0.1855	0.1115	-0.0823
C116	0.7801	0.3056	-0.4000
C117	0.7525	0.2627	-0.4245
C118	0.7179	0.2892	-0.4663
N119	0.6888	0.3549	-0.2657
H120	0.6946	0.7381	1.3842
H121	0.5659	0.3864	-0.4598

H122	0.6211	0.3603	-0.4780
H123	0.6732	0.4581	0.2978
H124	0.6195	0.4810	0.3329
H125	0.7613	0.2378	-0.2227
H126	0.6995	0.2571	-0.4645
C127	0.4068	0.5736	0.7378
C128	0.3995	0.6246	0.8366
C129	0.3701	0.6318	0.8986
C130	0.3469	0.5887	0.8554
C131	0.3543	0.5376	0.7651
C132	0.3841	0.5298	0.7113
C133	0.6752	0.7466	1.1704
C134	0.2727	0.6615	0.9423
C135	0.2486	0.6187	0.9871
C136	0.2125	0.6431	0.9044
N137	0.1794	0.7199	0.9774
H138	0.2075	0.0981	0.1027
H139	0.0634	0.7916	0.4195
H140	0.1170	0.7387	0.6097
H141	0.1509	0.8372	1.4038
H142	0.0980	0.8901	1.2094
H143	0.2589	0.6056	1.2199
H144	0.1954	0.6127	0.9453
H145	0.7629	0.8103	0.6778
H146	0.7541	0.9020	1.0814
H147	0.6920	0.8818	0.8431
H148	0.2736	0.1756	-0.6031
H149	0.2611	0.2657	-0.2083
H150	0.1994	0.2446	-0.4499
H151	0.2199	0.6829	1.3137
H152	0.2303	0.7536	0.8394
H153	0.2926	0.7419	1.1052
H154	0.7308	0.3075	-0.0147
H155	0.7395	0.3988	-0.4085
H156	0.8015	0.3807	-0.1701
H157	0.2312	0.1953	-0.0057
H158	0.2536	0.1003	-0.0210
H159	0.2955	0.1755	0.0596
H160	0.7210	0.8306	1.2776
H161	0.7464	0.7383	1.2765
H162	0.7878	0.8147	1.3443
H163	0.7734	0.3276	-0.6083
H164	0.7490	0.2346	-0.6127

H165	0.7067	0.3098	-0.6802
H166	0.2621	0.6751	0.7125
H167	0.2467	0.5820	0.8463
H168	0.2011	0.6527	0.6666
H169	0.9597	0.8664	0.8193
H170	0.9222	1.0218	0.4564
H171	0.0312	0.1335	-0.2212
H172	0.0692	-0.0212	0.1457
H173	0.9167	0.0689	0.0950
H174	0.9743	0.1611	-0.2800
H175	0.0161	0.8378	0.8692
H176	0.0739	0.9305	0.5002
C177	0.0290	0.0969	-0.1089
C178	0.0551	0.0580	-0.0265
C179	0.0511	0.0111	0.1179
C180	0.0240	0.0053	0.2155
C181	0.9410	0.0749	0.0762
C182	0.9683	0.0382	0.1987
C183	0.9975	0.0444	0.1258
C184	0.9998	0.0895	-0.0441
C185	0.9728	0.1269	-0.1478
C186	0.9433	0.1190	-0.0912
C187	-0.0069	0.9549	0.4663
C188	-0.0093	0.9097	0.6358
C189	0.0175	0.8719	0.7362
C190	0.0470	0.8796	0.6791
C191	0.0495	0.9242	0.5151
C192	0.0222	0.9611	0.3935
C193	0.4373	0.5259	0.4509
C194	0.4664	0.5147	0.3849
C195	0.4952	0.5495	0.5083
C196	0.4950	0.5917	0.7085
C197	0.4667	0.5985	0.7874
C198	0.4374	0.5661	0.6580
C199	0.5233	0.6264	0.8330
C200	0.5520	0.6190	0.7644
C201	0.5529	0.5766	0.5756
C202	0.5244	0.5421	0.4367
C203	0.4677	0.4699	0.2011
C204	0.4970	0.4626	0.1295
C205	0.4984	0.4179	-0.0535
C206	0.4709	0.3815	-0.1662
C207	0.4423	0.3882	-0.0945

C208	0.4410	0.4312	0.0895
C209	0.5276	0.4096	-0.1185
C210	0.5549	0.4467	-0.0192
C211	0.5520	0.4929	0.1416
C212	0.5247	0.4996	0.2375
H213	0.4136	0.5050	0.3363
H214	0.4680	0.6286	0.9545
H215	0.5231	0.6589	0.9842
H216	0.5768	0.5707	0.5501
H217	0.4716	0.3478	-0.3092
H218	0.4185	0.4332	0.1399
H219	0.5290	0.3734	-0.2425
H220	0.5711	0.5241	0.1834
C221	0.9667	0.9942	0.3788
C222	0.9619	0.9029	0.7059
C223	0.9361	0.9425	0.6296
C224	0.9399	0.9890	0.4814

Table S8 Atomistic coordinates for the refined unit cell parameters for TFPPer-PDA COF via Pawley refinement. Space group: $P6$; $a = b = 51.9929 \text{ \AA}$, $c = 3.4400 \text{ \AA}$, $\alpha = 90.0000^\circ$, $\beta = 90.0000^\circ$, and $\gamma = 120.0000^\circ$. Pawley-refined PXRD profile confirmed the correctness of the peak assignment as evident by a small difference with R_{wp} and R_p values of 1.14% and 2.79%, respectively.

C1	0.4730	0.0006	0.5707
C2	0.4728	0.5007	0.5584
C3	0.5006	0.5278	0.5829
C4	0.5027	0.5561	0.6231
C5	0.5299	0.5835	0.6019
C6	0.5560	0.5816	0.5729
C7	0.5553	0.5541	0.5704
C8	0.5823	0.5536	0.5669
C9	0.5829	0.5268	0.5363
C10	0.5549	0.5003	0.5170
C11	0.5307	0.6114	0.6054
C12	0.3898	0.4736	0.5278
C13	0.6121	0.5016	0.6610
C14	0.6389	0.5010	0.6536
C15	0.6654	0.5257	0.5240
C16	0.6641	0.5507	0.3923
C17	0.6371	0.5508	0.3900
C18	0.5557	0.6379	0.7398
C19	0.5568	0.6656	0.7300
C20	0.5325	0.6678	0.5965
C21	0.5072	0.6417	0.4682
C22	0.5065	0.6143	0.4684
N23	0.6903	0.5234	0.5346
C24	0.7192	0.5441	0.4846
C25	0.7418	0.5365	0.5004
N26	0.5353	0.6953	0.5951
C27	0.5148	0.7037	0.5392
C28	0.7721	0.5593	0.5049
C29	0.7951	0.5524	0.5204
C30	0.7886	0.5225	0.5292
C31	0.7584	0.4997	0.5241
C32	0.7354	0.5066	0.5110
H33	0.4840	0.5571	0.6755
H34	0.5763	0.6007	0.5504
H35	0.6018	0.5734	0.5890

H36	0.5550	0.4811	0.4644
H37	0.5940	0.4835	0.7718
H38	0.6391	0.4825	0.7492
H39	0.6828	0.5689	0.2922
H40	0.6374	0.5691	0.2807
H41	0.5736	0.6375	0.8509
H42	0.5755	0.6841	0.8250
H43	0.4891	0.6424	0.3666
H44	0.4880	0.5965	0.3592
H47	0.7777	0.5812	0.4976
H48	0.8166	0.5696	0.5233
H49	0.7527	0.4778	0.5302
H50	0.7139	0.4894	0.5079

Table S9. Cohesive energy values (E_c) for the TFPPer-PDA-CHDA-COF and TFPPer-PDA-CHDA-COF in the eclipsed stacking structures according to the DFT calculation.

	Interlayer Distance (Å)	LJ Energy (a.u.)	Per Layer Stabilization (kcal/mol)	E_c (kcal/mol)
TFPPer-PDA-CHDA-COF (kgm)	3.44	3.1061	-193.11	-64.37
TFPPer-PDA-CHDA-COF (sql)	3.41	2.0491	-138.33	-69.16
TFPPer-PDA-COF (kgm)	3.59	2.6737	-229.16	-76.39
TFPPer-PDA-COF (sql)	3.59	1.7973	-148.66	-74.33

Table S10. Comparison with some previously reported limits of detection for Fe³⁺, picric acid and phenyl glyoxylic acid.

Sample name	Wavelength	Solvent	Stern-Volmer Quenching Rate Constant (K_{sv})	Limit of Detection (LOD)	Reference
Detection for Fe ³⁺					
ETTA-CHDA COF	544 nm	THF	$2.00 \times 10^4 \text{ M}^{-1}$	680 ppb	Our Work
HMQC-MG	470 nm	water	n/a	0.199 μM	<i>ACS Appl. Polym. Mater.</i> 2020 , 2 (8), 3621–3631
JUC-557 nanosheet	514	ethanol /water = 1 : 9	$1.98 \times 10^4 \text{ M}^{-1}$	706 ppb	CCS Chem. 2022 , DOI:10.31635/ccsche m.022.202
COP-1	570 nm	<i>N,N</i> -dimethylacetamide	n/a	0.42 μM	<i>Chem. Commun.</i> 2019 , 55 (82), 12328–12331
Detection for Picric Acid					
ETTA-CHDA COF	544 nm	THF	$3.04 \times 10^5 \text{ M}^{-1}$	188 ppb	Our Work
USTC-7	370 nm	CHCl ₃	$4.90 \times 10^4 \text{ M}^{-1}$	2.78×10^{-4} mM	<i>Chem. Commun.</i> 2016 , 52 (33), 5734–5737
Py-azine COF	522 nm	CH ₃ CN	$7.8 \times 10^4 \text{ M}^{-1}$	n/a	<i>J. Am. Chem. Soc.</i> 2013 , 135 (46), 17310–17313

PI-COF	500 nm	ethanol	$1 \times 10^7 \text{ M}^{-1}$	$0.25 \mu\text{M}$	<i>ACS Appl. Mater. Interfaces</i> 2017 , <i>9</i> (15), 13415–13421
[Cd(NDC)0.5(PCA)]·Gx	384 nm	CH ₃ CN	$3.5 \times 10^4 \text{ M}^{-1}$	n/a	<i>Angew. Chem. Int. Ed.</i> 2013 , <i>52</i> (10), 2881–2885
Detection for Phenyl Glyoxylic Acid					
ETTA-CHDA COF	544 nm	THF	$2.83 \times 10^5 \text{ M}^{-1}$	134 ppb	Our Work
Tb-MOF 1	546 nm	water	$74.38 \times 10^{-3} \text{ M}^{-1}$	1.05×10^{-4} mg/mL	<i>ACS Appl. Mater. Interfaces</i> 2021 , <i>13</i> (28), 33546–33556.
Zn-PBA	422 nm	water	$1.26 \times 10^3 \text{ M}^{-1}$	1.67×10^{-3} M	<i>Appl. Organomet. Chem.</i> 2022 , <i>36</i> (1), e6468.
Eu@MOFs	322 nm	CH ₃ CN	n/a	1.012 ppm	<i>Biosens. Bioelectron.</i> 2017 , <i>97</i> , 299–304.

Section E: References

1. Jiang, S.; Bacsa, J.; Wu, X.; Jones, J. T. A.; Dawson, R.; Trewin, A.; Adams, D. J.; Cooper, A. I. Selective Gas Sorption in a [2+3] 'Propeller' Cage Crystal. *Chem. Commun.* **2011**, *47*, 8919–8921.
2. Jin, E.; Asada, M.; Xu, Q.; Dalapati, S.; Addicoat Matthew, A.; Brady Michael, A.; Xu, H.; Nakamura, T.; Heine, T.; Chen, Q.; Jiang, D. Two-Dimensional sp² Carbon-Conjugated Covalent Organic Frameworks. *Science* **2017**, *357*, 673–676.
3. Jin, E.; Li, J.; Geng, K.; Jiang, Q.; Xu, H.; Xu, Q.; Jiang, D. Designed Synthesis of Stable Light-emitting Two-Dimensional sp² Carbon-Conjugated Covalent Organic Frameworks. *Nat. Commun.* **2018**, *9*, 4143.
4. Jin, E.; Lan, Z.; Jiang, Q.; Geng, K.; Li, G.; Wang, X.; Jiang, D. 2D sp² Carbon-Conjugated Covalent Organic Frameworks for Photocatalytic Hydrogen Production from Water. *Chem* **2019**, *5*, 1632–1647.
5. Zhuang, X.; Zhao, W.; Zhang, F.; Cao, Y.; Liu, F.; Bi, S.; Feng, X. A Two-Dimensional Conjugated Polymer Framework with Fully sp²-Bonded Carbon Skeleton. *Polym. Chem.* **2016**, *7*, 4176–4181.
6. Chen, R.; Shi, J.-L.; Ma, Y.; Lin, G.; Lang, X.; Wang, C. Designed Synthesis of a 2D Porphyrin-Based sp² Carbon-Conjugated Covalent Organic Framework for Heterogeneous Photocatalysis. *Angew. Chem. Int. Ed.* **2019**, *58*, 6430–6434.
7. Xu, S.; Wang, G.; Biswal, B. P.; Addicoat, M.; Paasch, S.; Sheng, W.; Zhuang, X.; Brunner, E.; Heine, T.; Berger, R.; Feng, X. A Nitrogen-Rich 2D sp²-Carbon-Linked Conjugated Polymer Framework as a High-Performance Cathode for Lithium-Ion Batteries. *Angew. Chem. Int. Ed.* **2019**, *58*, 849–863.
8. Ascherl, L.; Evans, E. W.; Gorman, J.; Orsborne, S.; Bessinger, D.; Bein, T.; Friend, R. H.; Auras, F. Perylene-Based Covalent Organic Frameworks for Acid Vapor Sensing. *J. Am. Chem. Soc.* **2019**, *141*, 15693–15699.
9. Xu, X.; Zhang, S.; Xu, K.; Chen, H.; Fan, X.; Huang, N. Janus Dione-Based Conjugated Covalent Organic Frameworks with High Conductivity as Superior Cathode Materials. *J. Am. Chem. Soc.* **2022**, *145*, 1022–1030.
10. Jin, E.; Geng, K.; Lee, K. H.; Jiang, W.; Li, J.; Jiang, Q.; Irle, S.; Jiang, D. Topology-Templated Synthesis of Crystalline Porous Covalent Organic Frameworks. *Angew. Chem. Int. Ed.* **2020**, *59*, 12162–12169.
11. Porrès, L.; Holland, A.; Pålsson, L.-O.; Monkman, A. P.; Kemp, C.; Beeby, A. Absolute Measurements of Photoluminescence Quantum Yields of Solutions using an Integrating Sphere. *J. Fluoresc.* **2006**, *16*, 267–273.

12. Lee, C.; Yang, W.; Parr, R. G. Development of the Colle-Salvetti Correlation-Energy Formula into a Functional of the Electron Density. *Phys. Rev. B* **1988**, *37*, 785.
13. Becke, A. D. Density-Functional Thermochemistry. IV. A New Dynamical Correlation Functional and Implications for Exact-Exchange Mixing. *J. Phys. Chem. C* **1996**, *104*, 1040–1046.
14. Hourahine, B.; Sanna, S.; Aradi, B.; Köhler, C.; Niehaus, T.; Frauenheim, T. Self-Interaction and Strong Correlation in DFTB. *J. Phys. Chem. A* **2007**, *111*, 5671–5677.
15. Elstner, M.; Porezag, D.; Jungnickel, G.; Elsner, J.; Haugk, M.; Frauenheim, T.; Suhai, S.; Seifert, G. Self-Consistent-Charge Density-Functional Tight-Binding Method for Simulations of Complex Materials Properties. *Phys. Rev. B* **1998**, *58*, 7260.
16. Hosokawa, F.; Shinkawa, T.; Arai, Y.; Sannomiya, T. Benchmark Test of Accelerated Multi-Slice Simulation by GPGPU. *Ultramicroscopy* **2015**, *158*, 56–64.